

Density, Speed of Sound, and Viscosity Measurements of Reference Materials for Biofuels

Arno Laesecke,^{*,†} Tara J. Fortin,[†] and Jolene D. Splett[‡]

[†]Material Measurement Laboratory Thermophysical Properties Division and [‡]Information Technology Laboratory Statistical Engineering Division, National Institute of Standards and Technology, 325 Broadway, Boulder, Colorado 80305-3328, United States

S Supporting Information

ABSTRACT: Measurements of density, speed of sound, and viscosity have been carried out on liquid certified reference materials for biofuels as a function of temperature at ambient pressure. The samples included anhydrous and hydrated bioethanol and two biodiesel fuels from different feedstocks, soy and animal fat. The ethanol samples were measured from a maximum temperature of 60 to 5 °C (speed of sound) and to −10 °C (density and viscosity), respectively. The biodiesel samples were characterized from 100 °C (density and viscosity) and from 70 °C (speed of sound) to 10 °C (animal fat-based) and 5 °C (soy-based). Densities were measured with two vibrating-tube instruments of different accuracy. The speeds of sound were measured with a propagation-time method in an acoustic cell that was combined with one of the densimeters. Viscosities were measured with an open gravitational capillary viscometer and with a rotating concentric cylinder viscometer, according to Stabinger. The measurement results are reported with detailed uncertainty analyses.

1. INTRODUCTION

The mandated increased utilization of transportation fuels derived from biological feedstocks is a significant transition for an industry that has operated on petroleum feedstocks for decades. Perspectives and ramifications of this transition have been discussed by Knothe.¹ At the molecular level of the fuels, the transition is from largely nonpolar hydrocarbon constituents of gasoline and diesel to polar compounds such as alcohols and fatty acid methyl esters (FAME). While the properties of nonpolar compounds depend only on their molecular size and shape, the properties of polar compounds are additionally influenced by their intramolecular charge distribution and the resulting electrostatic interactions between the molecules. These can range from increased local order due to preferred orientations to the formation of hydrogen bonds and associates. Because of these molecular attractions, the macroscopic properties of polar compounds are often similar in magnitude to those of considerably larger nonpolar compounds. They have profound practical consequences for the utilization of biofuels. For instance, the less favorable low-temperature properties of biodiesel are an expression of the higher polarity of the constituent compounds in this fuel.²

Measurement needs arising from the transition to a new class of fuel materials are being addressed by initiatives of national metrology institutes.^{3–6} This report presents measurement results that were obtained at the National Institute of Standards and Technology (NIST) Thermophysical Properties Division at Boulder, Colorado. The measured biofuel liquids were the following:

- Inmetro anhydrous bioethanol AEAC (álcool etílico anhidratado combustível) (The National Institute of Metrology, Standardization and Industrial Quality, Santa Alexandrina St. 416, Rio Comprido, Rio de Janeiro, RJ 20261-232, Brazil, <http://www.inmetro.gov.br/>)

- Inmetro hydrated bioethanol AEHC (álcool etílico hidratado combustível, azeotrope of 95.57 wt % ethanol with 4.43 wt % water)
- NIST Standard Reference Material (SRM) 2772 B100 Biodiesel (soy-based)⁷
- NIST Standard Reference Material 2773 B100 Biodiesel (animal fat-based)⁸

The chemical compositions of the biodiesel samples as given in the SRM certificates are shown in Figure 1. All samples were provided by the NIST Analytical Chemistry Division in Gaithersburg, Maryland, and used as received. The measured properties were density, speed of sound, and viscosity as a function of temperature at the ambient pressure of approximately 0.083 MPa corresponding to the altitude of 1633 m above sea level of Boulder, Colorado.

The following parts of this report discuss the instruments and methods that were used for the measurements including uncertainty assessments. The measurement results are documented in tables and graphs.

2. INSTRUMENTS

Three apparatuses were used for the measurements reported here. Two of them were combination instruments where two properties are measured simultaneously on the same sample. A density and sound speed analyzer DSA 5000 from Anton Paar USA, Inc., Ashland, Virginia was used for measurements of these two properties in the temperature range 5 to 70 °C. (To describe materials and experimental procedures adequately, it is occasionally necessary to identify commercial products by manufacturers' names or labels. In no instance does such identification imply endorsement by the National Institute of

Received: October 24, 2011

Revised: January 13, 2012

Published: February 10, 2012

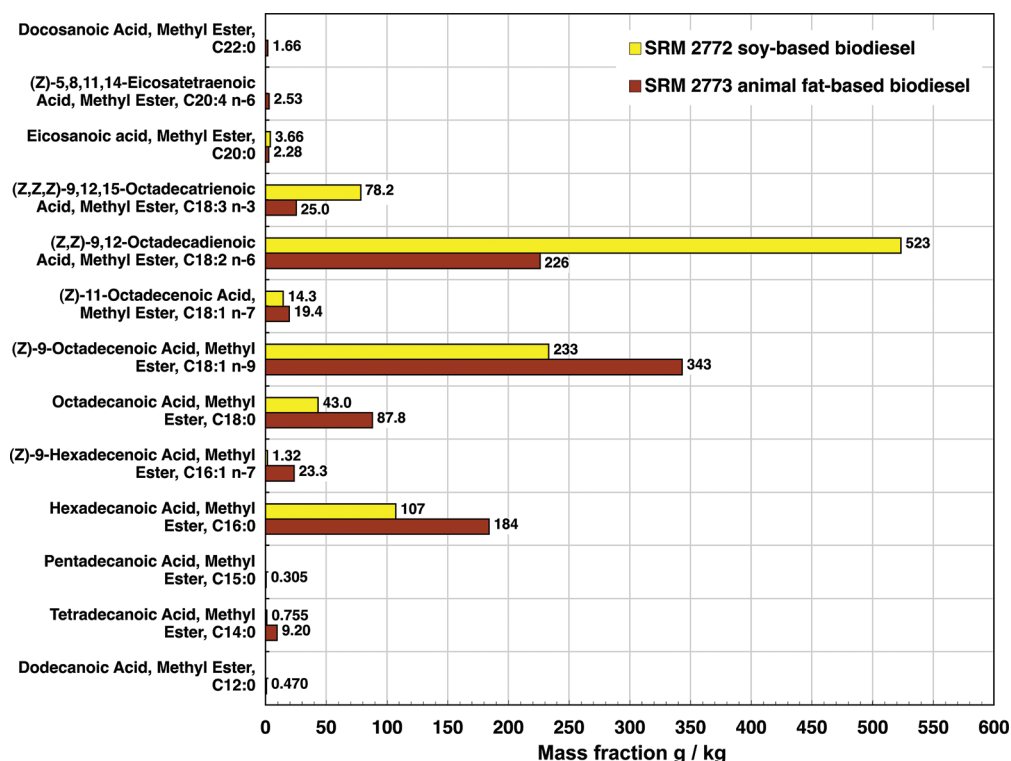


Figure 1. Compositions of NIST B100 Biodiesel Standard Reference Materials.

Standards and Technology, nor does it imply that the particular product or equipment is necessarily the best available for the purpose.) The densimeter in this instrument will be denoted henceforth as “densimeter 1”. An automated open gravitational glass capillary viscometer “miniAV” from Cannon Instrument Company, State College, Pennsylvania, was used for kinematic viscosity measurements in the range from 20 to 60 °C (bioethanols) or 100 °C (biodiesels). This viscometer will be denoted henceforth as “viscometer 1”. A viscodensimeter SVM 3000 from Anton Paar USA, Inc. was used for density and viscosity measurements in a combined temperature range from –10 to 100 °C. This instrument consists of a vibrating-tube densimeter in series with a rotating concentric cylinder viscometer according to Stabinger for dynamic viscosity measurements. The densimeter in this instrument will be denoted henceforth as “densimeter 2” and the viscometer as “viscometer 2”.

A difference in the operation of these three apparatuses needs to be pointed out. Sample liquids are injected with syringes into the combination instruments in volumes of about 3 mL per charge. The measurements are programmed scans from a maximum temperature in decrements of 5 °C to a minimum temperature. The scans were repeated five times with fresh sample aliquots injected before each so that the reproducibility of the measurements was obtained.⁹ The measurements with the capillary viscometer were carried out on one sample aliquot of about 15 mL in programmed scans from 20 °C and increments of 5 °C to the respective maximum temperature of 60 °C (bioethanols) or 100 °C (biodiesels). At each temperature, the instrument was programmed to repeat efflux time measurements until three consecutive tests agreed within $\pm 0.25\%$. The standard deviations of these measurements yield the repeatability of measurements with this instrument.

We note also that a careful cleaning procedure was adopted for the density and sound speed analyzer after it was found that

sample liquids could become trapped in the acoustic cell. Solvents to purge the manifold and the cells were selected for optimal miscibility with each sample liquid. To promote miscibility further, the manifold temperature was raised to 40 °C for purging with acetone, to 50 °C for purging with hexanes, and to 70 °C for purging with *n*-decane and deionized water. In certain cases, sequential purges with two or more solvents were performed. Final air drying of the manifold was always carried out at 70 °C. A critical improvement over the recommendations of the manufacturer was the requirement of three consecutive water checks reproducing the density and the speed of sound of water at 20 °C with a relative deviation of less than ± 0.00010 . One or two water checks within this margin are not sufficient to ensure the complete removal of a sample from the acoustic cell.

Further details of the instruments, the sensing techniques, and the measurement protocols will be described in the following sections.

2.1. Densimeters. Both densimeters implement the vibrating-tube method with resonators of borosilicate glass. Densimeter 1 is of the same high precision as that in the Anton Paar model DMA 5000, which is widely used to characterize SRMs. The density resolution is $0.001 \text{ kg}\cdot\text{m}^{-3}$. Densimeter 1 and the acoustic cell for sound speed measurements are in an isothermal block, the temperature of which is controlled with thermoelectric Peltier elements and measured with an embedded 100 Ω platinum resistance thermometer. The resolution of the thermometer and its uncertainty are stated by the manufacturer as 1 mK and 10 mK, respectively. The temperature range of the thermostating system is from 5 to 70 °C.

Densimeter 1 was originally adjusted by the manufacturer with deionized water and air. Calibrations were performed in February 2006 with NIST SRM 211d toluene. The three densities of the liquid at 15 °C, 20 °C, and 25 °C at normal atmospheric pressure, which were certified at that time as

standard reference data, were reproduced within their certified uncertainties. In 2008, toluene was expanded as a liquid density standard over the temperature range -50 to 150 °C with pressures from 0.1 to 30 MPa.¹⁰ Densimeter 1 was readjusted with deionized water and air prior to the biofuels measurements. Calibration measurements with these two fluids and with NIST SRM 211d toluene were repeated before and after the biofuels measurements. The reference densities of water¹¹ and air¹² as calculated with the NIST REFPROP software¹³ were reproduced within $\pm 0.01\%$. Figure 2 shows the relative deviations of the

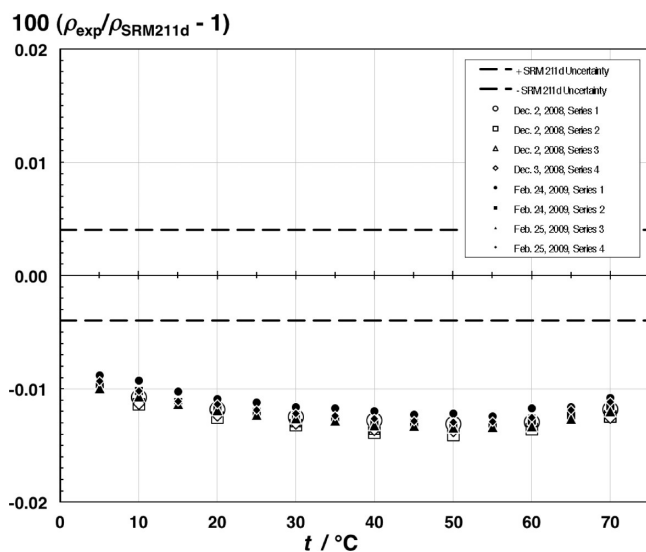


Figure 2. Relative deviations of densities of toluene measured in densimeter 1 from reference values of NIST Standard Reference Material 211d toluene as a function of temperature.

calibration measurement result from the reference data of NIST SRM 211d toluene over the temperature range of the instrument. They confirm a systematic offset of densimeter 1 at the density of toluene ranging between -0.009% at 5 °C and -0.014% at 50 °C. The measured densities of the biodiesel samples were corrected for this offset because they were close to the densities of toluene, exceeding those from about $10 \text{ kg}\cdot\text{m}^{-3}$ at 5 °C to about $25 \text{ kg}\cdot\text{m}^{-3}$ at 70 °C. Details of this correction are given in Appendix A1 in the Supporting Information.

Densimeter 2 was adjusted in reference to the density of air and to the densities of certified viscosity reference standards (CVRS) N14 and N44 from Cannon Instrument Company at temperatures from 20 to 100 °C with increments of 20 °C. At $0.1 \text{ kg}\cdot\text{m}^{-3}$, the resolution of densimeter 2 is 2 orders of magnitude lower than that of densimeter 1. The densities of the biofuels measured in densimeter 2 are included in this report for orientation, because they extend to lower temperatures for the bioethanol samples and to higher temperatures for the biodiesel liquids than the densities measured with densimeter 1. This information is valuable for the biofuels industry.

2.2. Speed of Sound Measurement. The acoustic cell for speed of sound measurements connects in series with densimeter 1. The cell has a circular cylindrical cavity of 8 mm diameter and 5 mm thickness that is sandwiched between the transmitter and receiver. The speed of sound is determined by measuring the propagation time of ultrasound signals with a frequency of 3.5 MHz from the transmitter to the receiver. The temperature of the speed of sound measurements is determined with the same thermometer that measures the temperature of

densimeter 1. The speed of sound measurement system was calibrated and adjusted with deionized water and air with reference values of the speed of sound of water¹¹ and air¹² calculated with the NIST REFPROP software.¹³

When the densimeter of the instrument was calibrated with NIST SRM 211d toluene, sound speed data were also obtained for this material. In the absence of certified values of the sound speed of toluene, results of Meier and Kabelac¹⁴ are used here as reference values. They were measured with an instrument with an estimated expanded uncertainty of 0.014%.¹⁵ At four temperatures in the range of the present instrument, the reference values were extrapolated to the ambient pressure of this laboratory by fitting the sound speeds along isotherms up to 10 MPa to polynomials and calculating values at 0.083 MPa from those. Figure 3 shows percent deviations of experimental

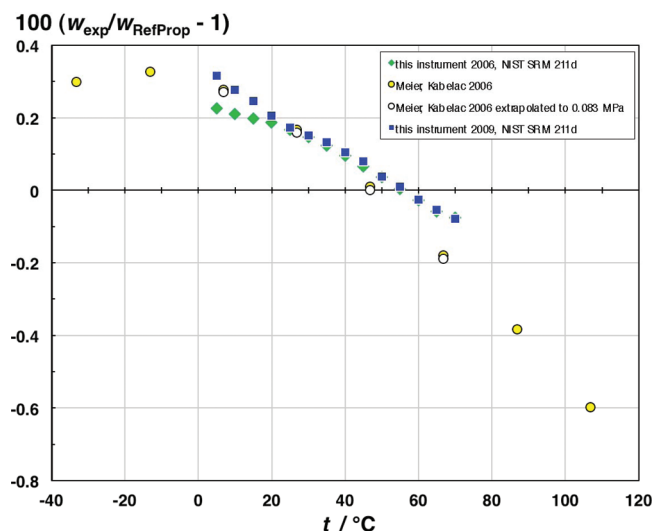


Figure 3. Relative deviations of measured speeds of sound of toluene from values calculated with the Helmholtz equation of state of Lemmon and Span¹⁶ as a function of temperature.

data relative to speed of sound values calculated with the fundamental equation of state by Lemmon and Span.¹⁶ The comparison includes two series of measurements with the present instrument that were recorded in February 2006 and February 2009 before and after the biofuel measurements. Agreement within the estimated uncertainty of the data of Meier and Kabelac occurred at 26.85 °C. At 5 °C, the lower limit of the instrument temperature range, the results of February 2009 are approximately 0.03% higher than the experimental value of Meier and Kabelac, while in February 2006 they were 0.06% lower. At 70 °C, the upper limit of the instrument temperature range, both results from this instrument are 0.13% higher than those of Meier and Kabelac. To put the uncertainty assessment in Appendix 2 of the Supporting Information to this report in perspective, we note that this corresponds to an absolute difference in the speed of sound of $1.47 \text{ m}\cdot\text{s}^{-1}$. Figure 3 shows also that all experimental data deviate systematically from the equation of state values with limiting values of 0.33% at -13.15 °C and -0.6% at 106.85 °C.

A number of density and speed of sound measurements that were performed with this instrument have been published previously.^{17–25}

2.3. Viscometers. **2.3.1. Open Gravitational Capillary Viscometer.** Viscosity measurements of the biofuel materials

were carried out at ambient pressure in the temperature range 20 to 100 °C with viscometer 1, an automated open gravitational capillary viscometer system. Figure 4 shows the

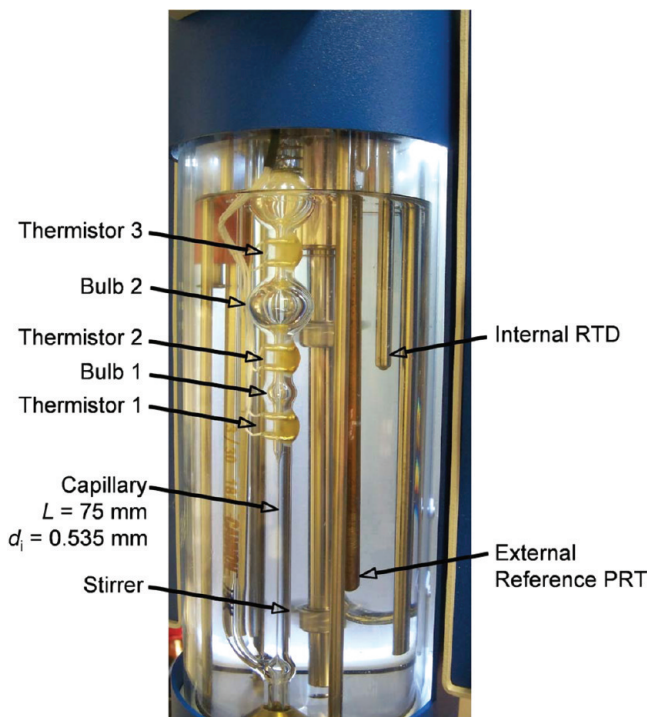


Figure 4. Dual-bulb capillary viscometer 1 in thermostating bath.

thermostating bath section of the instrument with the glass capillary, two timing bulbs, three thermistor sensors that detect the passing of menisci of sample liquids, a stirrer, and an internal temperature sensor, as well as an external platinum resistance thermometer (PRT). The main part of the flow impedance in this instrument is a suspended-level Ubbelohde glass capillary of 75 mm length and a nominal internal diameter of 0.535 mm. The viscometer has two timing bulbs above the straight vertical capillary section to use different volumes of the sample liquid in two different viscosity ranges. The lower timing bulb 1 with thermistor sensors 1 and 2 is used for liquids with kinematic viscosities (momentum diffusivities) in the approximate range from $3 \text{ mm}^2\cdot\text{s}^{-1}$ to $30 \text{ mm}^2\cdot\text{s}^{-1}$. In such measurements, the sample liquid drains only through the capillary section for the efflux time measurement, and the flow conforms largely to the assumptions of the Hagen–Poiseuille equation,²⁶ which are the following:

1. The capillary is straight and has a uniform circular cross section.
2. The fluid is incompressible, and its density is constant.
3. The fluid is Newtonian, and viscosity variations due to the pressure drop along the capillary are negligible.
4. The temperature of the fluid is constant, and heat generation due to viscous dissipation is negligible.
5. The flow is laminar and steady.
6. There is no slip at the wall of the capillary.

Liquids with kinematic viscosities lower than the crossover value of $3 \text{ mm}^2\cdot\text{s}^{-1}$ are measured by raising them above bulb 2 and recording the efflux time from when the liquid meniscus passes thermistor 3 until it passes thermistor 1 below bulb 1. In such measurements, bulb 1 becomes part of the flow

impedance in addition to the straight capillary section during that part of the efflux when the liquid meniscus is above bulb 1. When the liquid drains through both bulb 1 and the capillary, assumption 1 is no longer met while the liquid meniscus is between thermistors 2 and 3. Also, assumption 5 may no longer hold when the liquid meniscus passes from the upper bulb 2 through the constriction to bulb 1.

The viscosity range of the instrument is also expanded by measuring to efflux times shorter than 200 s. This is the lower limit recommended for most gravitational viscometers in ASTM Standard D446²⁷ so that kinetic energy conversion effects on the efflux can be neglected. The faster flow of the sample liquid at shorter efflux times requires accounting for these effects with the working equation

$$\nu = c\tau - \varepsilon/\tau^2 \quad (1)$$

for the kinematic viscosity ν and the efflux time τ . Parameter c arises from the Hagen–Poiseuille equation, and ε is the kinetic energy correction factor. They were determined for the two viscosity ranges with certified viscosity reference standards (CVRS) N.4, N1.0, S3, S6, N10, and N14 from Cannon Instrument Company at temperatures from 20 to 100 °C. As mentioned before, the measurement acceptance criterion for viscometer 1 was set to a maximum spread of three consecutively measured efflux times of less than 0.25%. The parameters in eq 1 were adjusted for each bulb to the reference values of the standards with efflux times in the range $40 \text{ s} \leq \tau \leq 110 \text{ s}$, because the associated viscosities covered those of the biofuels. The resulting viscosity–efflux time-relationships of both bulbs are shown in Figure 5 for efflux times up to 600 s.

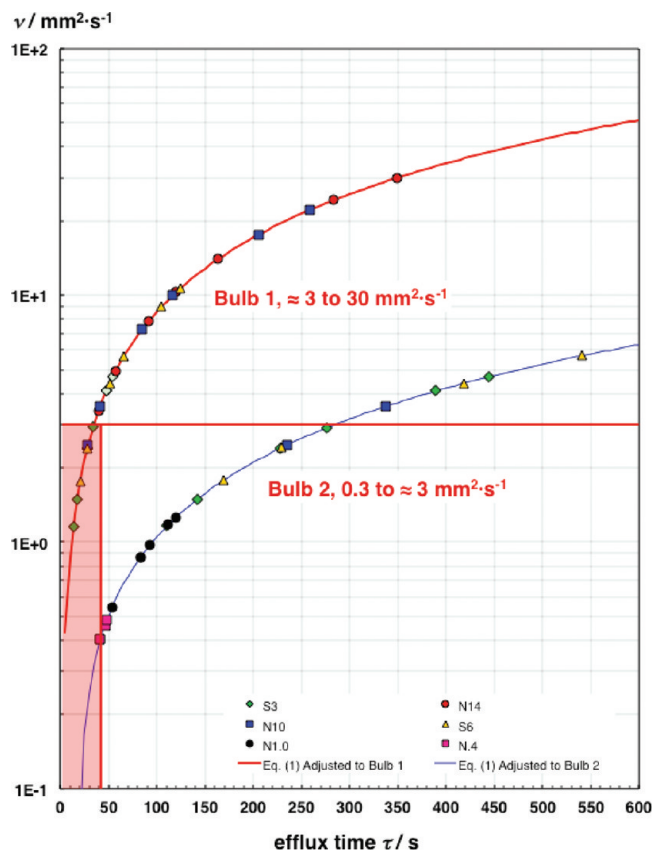


Figure 5. Viscosity–efflux time relationships for the two bulbs of viscometer 1.

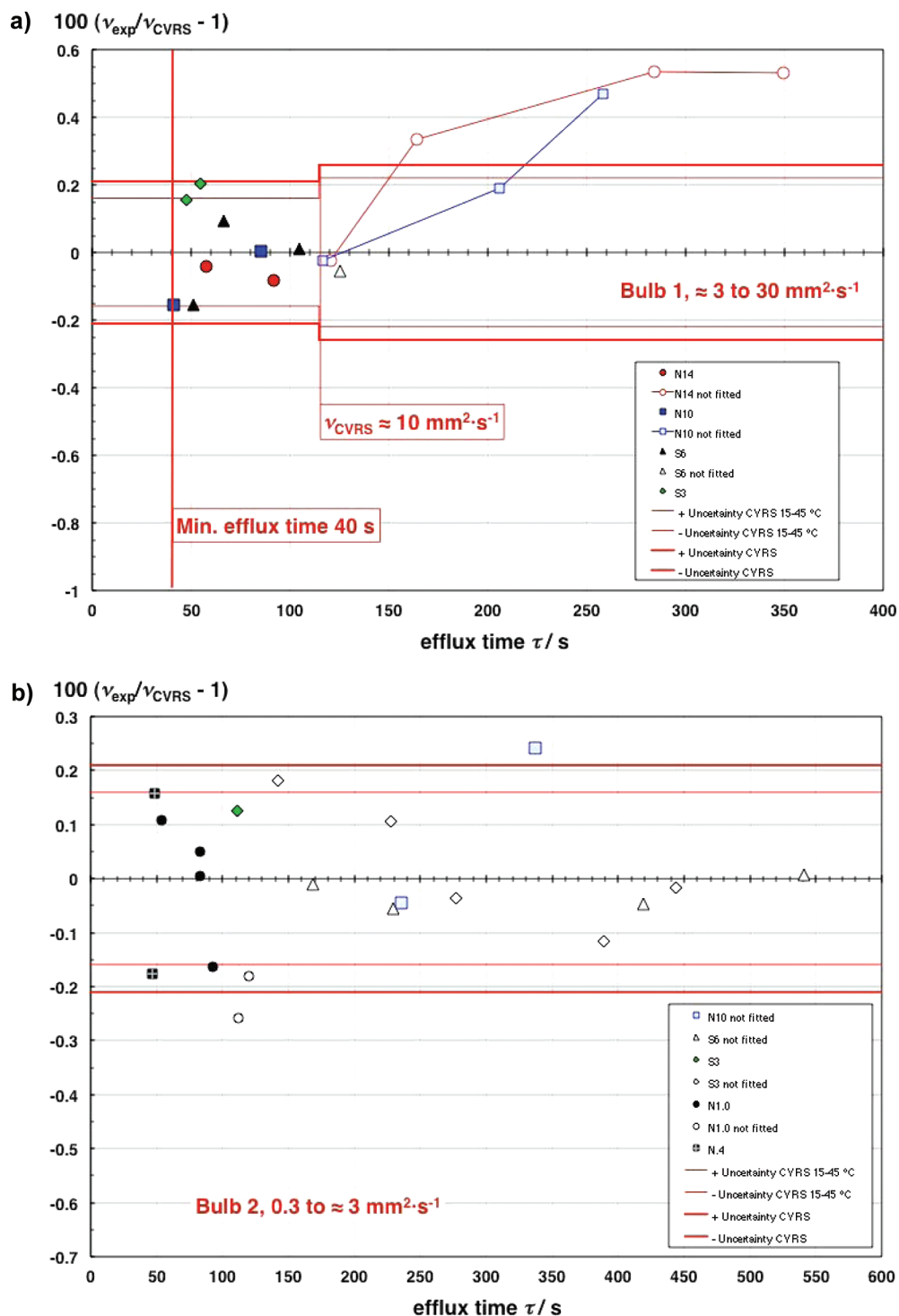


Figure 6. Relative deviations of adjusted working eq 1 from certified viscosity reference standards values for (a) bulb 1 of viscometer 1 and (b) bulb 2 of viscometer 1.

The parameter values c and ε and their uncertainties are listed in Appendix A3 in the Supporting Information. Note that, in contrast to the default value of zero of the manufacturer, parameter ε for bulb 1 is greater than zero and is statistically significant. The representation of the certified viscosity reference standard values by eq 1 with these parameter values is shown in Figure 6a for bulb 1 and Figure 6b for bulb 2. For bulb 1, the CVRS values in the fitted efflux time range are represented within their expanded uncertainties at the 95% confidence level of 0.16% for $\nu < 10 \text{ mm}^2\cdot\text{s}^{-1}$ or 0.22% for

$10 \text{ mm}^2\cdot\text{s}^{-1} \leq \nu < 100 \text{ mm}^2\cdot\text{s}^{-1}$ in the temperature range 15 to $45 \text{ }^\circ\text{C}$, and within 0.21% for $\nu < 10 \text{ mm}^2\cdot\text{s}^{-1}$ or 0.26% for $10 \text{ mm}^2\cdot\text{s}^{-1} \leq \nu < 100 \text{ mm}^2\cdot\text{s}^{-1}$ at other temperatures. The trend of the deviations suggests that eq 1 can be extrapolated to efflux times up to approximately 140 s . At higher efflux times, eq 1 deviates systematically from the CVRS values up to 0.54% . The curvature of the deviations from 40 s efflux time to 350 s has been observed in all our calibrations of bulb 1 and is interpreted as an indication that eq 1 does not describe completely the flow of liquids through bulb 1 and the capillary.

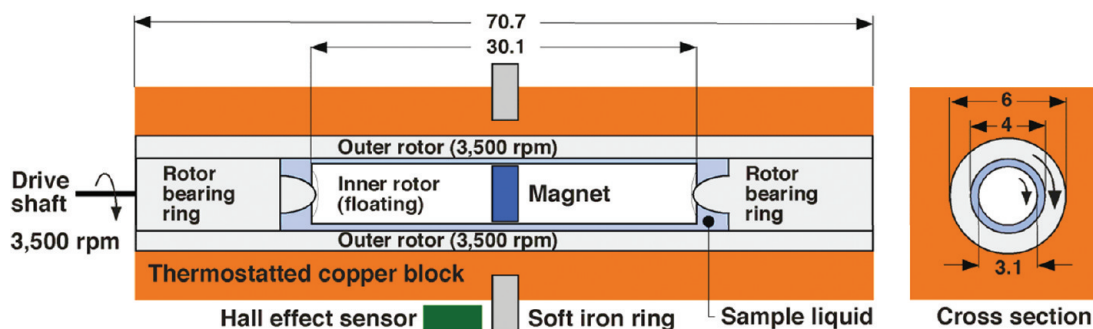


Figure 7. Schematic of the rotating concentric cylinder viscometer 2. Dimensions are given in millimeters. For details see text.

Either the kinetic energy correction term (ϵ/τ^2) needs to be modified or an additional term is needed in the working equation for this case. Conversely, Figure 6b, with the deviations for bulb 2, shows that eq 1 represents almost all CVRS values within their expanded uncertainties of 0.16% in the temperature range 15 to 45 °C and within 0.21% at other temperatures up to efflux times of 600 s, even when the parameters c and ϵ are adjusted to CVRS values only in the range $40 \text{ s} \leq \tau \leq 110 \text{ s}$. This is somewhat surprising, because the liquid flow through bulb 2 involves the nonstraight bulb 1 as a flow impedance in addition to the capillary. As will be seen in the results section below, it was observed in this work that measurements with bulb 2 generally appear to be more accurate than those with bulb 1.

The thermostating system and temperature measurement of viscometer 1 deserves special attention because its uncertainty contributes substantially to the uncertainty of the viscosity measurement. As shown in Figure 4, the glass capillary is mounted in a thermostating bath filled with silicone oil. The thermostat includes a stirrer, a heat pipe to a thermoelectric Peltier cooler at the top of the bath (not visible), an internal resistance temperature detector (RTD), and an external 100 Ω platinum resistance thermometer (PRT). The bath temperature is set between 20 and 100 °C with the operating software that is an integral part of the viscosity measurement system. The equilibration criterion was set to temperature control within $\pm 0.02 \text{ K}$. The resistance of the PRT is measured with an external ac bridge. The calibration of the PRT on the International Temperature Scale of 1990 was checked by comparison with a water triple point cell. The estimated uncertainty of the external reference PRT is 0.01 K. The temperature that is associated with a viscosity measurement during automatic operation is recorded with the internal RTD sensor. This has to be adjusted against the external reference PRT by entering a temperature offset in the instrument operating software. In our experience, this adjustment has to be repeated at least weekly. To account for this adjustment, an additional uncertainty of 0.01 K was included in the uncertainty budget. Third, although the thermal equilibration criterion was set to temperature control within $\pm 0.02 \text{ K}$, larger temperature fluctuations were observed that varied with the set point temperature. Considering also, that temperature gradients in the bath increase with higher temperature differences between bath and environment, an additional uncertainty ranging from 0.02 K at 20 °C (293.15 K) to 0.1 K at 100 °C (373.15 K) was included in the uncertainty budget of this viscometer. Further details are given in Appendix A3 in the Supporting Information.

Viscometer 1 includes a manifold with pneumatics and electronics to perform automated measurements at a series of up to ten temperatures as well as washing and drying the

capillary and bulbs with two different solvents when samples are changed. Hexanes and acetone were used as solvents in this work. After some measurements of certified viscosity reference standards with elevated viscosities, *n*-decane was used as the first solvent before hexanes and acetone were applied.

2.3.2. Rotating Concentric Cylinder Viscometer. Viscometer 2 is a rotating concentric cylinder viscometer according to Stabinger in series with a vibrating-tube cell for density measurements ("densimeter 2"). A schematic of the viscometer is shown in Figure 7. It consists of two horizontally mounted concentric cylinders in a thermostatted copper block. The outer cylinder is made of hastelloy and has a length of 70.7 mm, including the rotor bearing rings at both ends. Its outer diameter is 6 mm, and the diameter of the bore is 4 mm. Loosely longitudinally positioned by the rotor bearings in the outer cylinder is a titanium cylinder of 30.1 mm length and 3.1 mm diameter that contains a small magnet but is otherwise hollow. The sample liquid is injected into the annular gap of 0.45 mm width between the cylinders through bores in the rotor bearing rings. The minimum sample volume to fill the entire instrument including the densimeter and the viscometer is about 3 mL.

During viscosity measurements, the outer cylinder is rotated at $n_o = 3500 \text{ rpm}$ by an external electric motor via a drive shaft that is coupled to one of the rotor bearings. The shear at the inner wall of the rotating outer cylinder drags the sample liquid into rotation, which, in turn, transmits its angular momentum onto the floating inner cylinder. Without a braking action, all three components would rotate synchronously in stationary equilibrium after a certain acceleration time. For the concentric alignment of the inner cylinder with the outer rotor, the instrument appears to rely on the normal stress developed by the test liquid. Compounds of small molecular size may not exert sufficiently high stress to center the inner cylinder so that it will rotate out of alignment with the outer rotor. This may result in a systematic uncertainty of this measurement method at low viscosities.

To measure the viscosity of the test liquid, the inner cylinder is slowed by magnetic induction and the viscosity is obtained from the different number of revolutions of the outer and the inner rotors. For this purpose, the inner cylinder contains a small magnet, the rotation of which induces eddy currents in the copper block of the measuring cell that slow the inner cylinder to a lower number of revolutions than the outer cylinder. Magnetic coupling between the magnet and the soft iron ring keeps the inner cylinder in its axial position. The revolutions of the rotating field of the magnet in the inner cylinder n_i are measured with the Hall effect sensor, and the dynamic viscosity η of the sample is obtained from the ratio of the number of revolutions n_o/n_i and a working equation with 12 parameters

that accounts for the geometrical dimensions of the viscometer and for the influence of temperature on the electromagnetic eddy current sensing system. The parameter values are adjusted at 20 °C, 60 °C, and 100 °C, but the instrument can be used for measurements from 0 to 100 °C with the built-in thermoelectric thermostating system. Lower temperatures can be achieved if additional cooling is provided by an external circulator. Series of measurements can be programmed by entering tables of uneven temperatures or by entering bounds of a temperature interval and a temperature step. The temperature during the viscosity and density measurements is sensed by a small 100 Ω platinum resistance thermometer embedded in the thermostatted copper block. The uncertainty of the temperature measurement is quoted by the manufacturer as 20 mK.

The viscometer was calibrated and adjusted in two viscosity measuring ranges with certified viscosity reference standards from Cannon Instrument Company. The “regular” viscosity range extends from the viscosity of CVRS S3 at 100 °C (0.94 mPa·s) to the viscosity of CVRS N415 at 20 °C (1150 mPa·s). CVRS N14 and N44, with intermediate viscosities between those of S3 and N415, are also part of this adjustment. While viscosity standard S3 is produced from mineral oil, the standards N14, N44, and N415 are formulated from poly- α -olefins. An adjustment for “ultralow” viscosities below 3 mPa·s uses CVRS N.4 (a mixture of hexane isomers) at 20 °C, *n*-octane at 60 °C, and CVRS N1.0 (*n*-decane) at 100 °C, with nominal viscosities between 0.330 mPa·s and 0.367 mPa·s to determine three parameters of an additional term in the working equation of the instrument for that range. Both adjustments of viscometer 2 were performed in this laboratory before the biofuel measurements, so that the 15 reference viscosities of the standards were met within $\pm 0.35\%$. However, the viscosity of standard N44 at 20 °C (92 mPa·s) could only be reproduced with a smallest deviation of 0.59%. This viscosity is considerably higher than the highest viscosity of 8.489 mPa·s that was measured in the animal-fat based biodiesel 2773 at 10 °C. The lowest viscosity measured in this work was 0.5876 mPa·s for bioethanol AEAC at 60 °C.

Because viscometer 2 can be used to temperatures below 20 °C, the bioethanol samples were measured in this instrument to -10 °C and the biodiesel samples to 10 °C. While the uncertainty of these viscosity and density results cannot be corroborated by comparison with results from densimeter 1 and viscometer 1, these data are nevertheless included here because they are valuable for the biofuels industry.

3. RESULTS

3.1. Density Measurements. Results of the density measurements of the four sample liquids are listed in Table 1 for densimeter 1 and in Table 2 for densimeter 2. Included in the tables are estimated uncertainties, which have been calculated as described in Appendix A1 of the Supporting Information. The combined temperature range of the biodiesel measurements is from 5 to 100 °C. However, the NIST SRM 2773 B100 animal fat-based biodiesel froze at 5 °C and could be measured only to 10 °C. The measured temperature dependencies of the densities are illustrated in Figure 8. The density of NIST SRM 2772 B100 soy-based biodiesel is slightly higher than that of NIST SRM 2773 B100 animal fat-based biodiesel because it contains more unsaturated C18-fatty acids (linoleic and linolenic acid) methyl esters than the latter. The temperature dependencies are rather linear. The densities of AEHC hydrated bioethanol and AEAC anhydrous

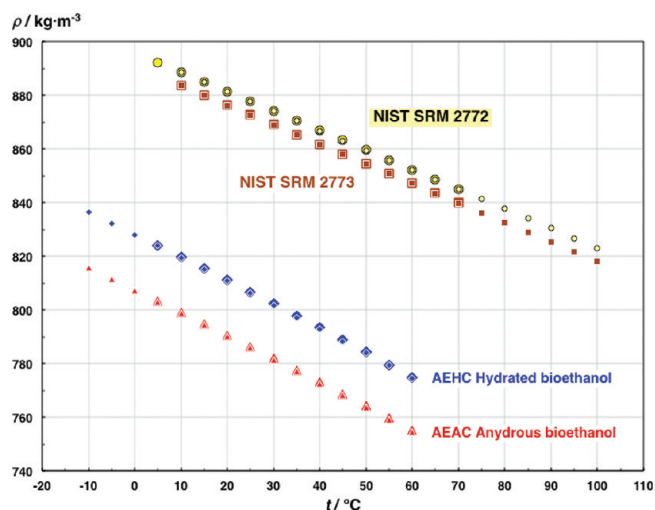


Figure 8. Measured densities of bioethanol materials and NIST B100 Biodiesel Standard Reference Materials as a function of temperature. Large symbols denote data measured with densimeter 1. Small symbols denote data measured with densimeter 2.

bioethanol were measured in a combined temperature range from -10 to 60 °C to avoid evaporation of the samples at higher temperatures. They are lower than the densities of the biodiesel samples and show steeper temperature dependencies with more curvature. This results from the polarities of water and ethanol molecules, which lead to associations by hydrogen bonding. As a result of these associations, the density of the hydrated bioethanol AEHC is approximately 20 $\text{kg}\cdot\text{m}^{-3}$ higher than that of AEAC anhydrous bioethanol. This effect of water on the density of water–ethanol mixtures is well-known.²⁸

Percent deviations of the densities measured with densimeter 2 from those measured with densimeter 1 are shown in Figure 9. The densities of AEAC anhydrous bioethanol from densimeter 2 are between 0.043% and 0.073% lower than those from densimeter 1. These deviations exceed the calculated relative expanded uncertainties of the data from densimeter 2. The deviations of the densimeter 2 data for AEHC hydrated bioethanol agree with those of densimeter 1 within their calculated relative expanded uncertainty from 5 to 20 °C, but then increase to a highest deviation of -0.098% at 35 °C. The course of these deviations appears systematic, but there is no obvious reason that would rationalize why they occurred for this sample liquid and not for the others. The density data from densimeter 2 for the biodiesel samples agree with those from densimeter 1 within their calculated relative expanded uncertainties, which range from 0.023% at 10 °C to 0.027% at 70 °C. It is noteworthy that the densities at 20 °C, which are currently on the certificates of NIST SRM 2772⁷ and NIST SRM 2773,⁸ are a statistical combination of the present results of densimeter 2 and of measurements carried out at Inmetro. They deviate from the results of densimeter 1 only by 0.002% and 0.006%, respectively. These deviations are within the calculated expanded uncertainty of the results of densimeter 1.

3.2. Speed of Sound Measurements. The results of the speed of sound measurements of the four sample liquids are listed in Table 3. Included in the table are estimated uncertainties that have been calculated as described in Appendix A2 of the Supporting Information. Figure 10 illustrates the temperature dependencies of the measured speeds of sound of the four samples from 5 to 70 °C. The speeds of sound increase in the

Table 1. Densities of Certified Biofuel Reference Materials and Their Uncertainties, as Measured with the Vibrating-Tube Densimeter 1 at Ambient Atmospheric Pressure (0.083 MPa)

AEAC anhydrous bioethanol								
temp. t , °C	avg density $\bar{\rho}$, kg·m ⁻³	combined standard uncertainty $u(\bar{\rho})$, kg·m ⁻³	effective degrees of freedom df	coverage factor k at 95% uncertainty	expanded uncertainty $U(\bar{\rho})$, kg·m ⁻³	relative expanded uncertainty $U(\bar{\rho})/\bar{\rho}$, %		
5	803.242	0.003	3	2.7769	0.008	0.001		
10	798.999	0.003	3	2.8452	0.009	0.001		
15	794.742	0.003	4	2.7520	0.007	0.001		
20	790.468	0.003	3	2.8229	0.008	0.001		
25	786.174	0.003	3	2.8107	0.008	0.001		
30	781.852	0.003	4	2.7572	0.007	0.001		
35	777.499	0.003	3	2.8459	0.009	0.001		
40	773.105	0.003	4	2.7444	0.007	0.001		
45	768.667	0.003	3	2.8042	0.008	0.001		
50	764.176	0.002	4	2.6141	0.006	0.001		
55	759.627	0.002	4	2.6195	0.006	0.001		
60	755.013	0.002	4	2.6335	0.006	0.001		
AEHC hydrated bioethanol								
temp. t , °C	avg density $\bar{\rho}$, kg·m ⁻³	combined standard uncertainty $u(\bar{\rho})$, kg·m ⁻³	effective degrees of freedom df	coverage factor k at 95% uncertainty	expanded uncertainty $U(\bar{\rho})$, kg·m ⁻³	relative expanded uncertainty $U(\bar{\rho})/\bar{\rho}$, %		
5	823.843	0.003	4	2.5966	0.009	0.001		
10	819.593	0.003	4	2.6012	0.009	0.001		
15	815.314	0.004	4	2.6141	0.009	0.001		
20	811.002	0.003	4	2.6066	0.009	0.001		
25	806.654	0.004	4	2.6153	0.009	0.001		
30	802.262	0.003	4	2.5983	0.009	0.001		
35	797.825	0.004	4	2.6320	0.010	0.001		
40	793.334	0.004	4	2.6240	0.010	0.001		
45	788.788	0.004	4	2.6350	0.010	0.001		
50	784.177	0.004	4	2.6176	0.009	0.001		
55	779.498	0.004	4	2.6176	0.009	0.001		
60	774.746	0.004	4	2.6727	0.010	0.002		
NIST SRM 2772 B100 biodiesel (soy-based)								
temp. t , °C	avg density $\bar{\rho}$, kg·m ⁻³	toluene correction C , kg·m ⁻³	corrected density $\bar{\rho}$, kg·m ⁻³	combined standard uncertainty $u(\bar{\rho})$, kg·m ⁻³	effective degrees of freedom df	coverage factor k at 95% uncertainty	expanded uncertainty $U(\bar{\rho})$, kg·m ⁻³	relative expanded uncertainty $U(\bar{\rho})/\bar{\rho}$, %
5	892.243	0.051	892.294	0.031	16	2.1151	0.066	0.0074
10	888.579	0.054	888.633	0.031	16	2.1160	0.066	0.0074
15	884.920	0.060	884.980	0.031	15	2.1270	0.066	0.0075
20	881.268	0.065	881.333	0.032	15	2.1278	0.069	0.0078
25	877.622	0.066	877.689	0.032	15	2.1281	0.069	0.0078
30	873.981	0.067	874.048	0.033	15	2.1284	0.071	0.0081
35	870.345	0.067	870.411	0.033	15	2.1275	0.071	0.0081
40	866.709	0.069	866.777	0.034	14	2.1416	0.073	0.0084
45	863.077	0.067	863.144	0.034	14	2.1416	0.073	0.0085
50	859.444	0.068	859.512	0.035	14	2.1416	0.075	0.0088
55	855.813	0.066	855.880	0.035	14	2.1421	0.075	0.0088
60	852.185	0.061	852.246	0.036	13	2.1577	0.078	0.0092
65	848.557	0.056	848.613	0.037	13	2.1579	0.080	0.0095
70	844.927	0.049	844.977	0.037	13	2.1577	0.080	0.0095
NIST SRM 2773 B100 biodiesel (animal fat-based)								
temp. t , °C	avg density $\bar{\rho}$, kg·m ⁻³	toluene correction C , kg·m ⁻³	corrected density $\bar{\rho}$, kg·m ⁻³	combined standard uncertainty $u(\bar{\rho})$, kg·m ⁻³	effective degrees of freedom df	coverage factor k at 95% uncertainty	expanded uncertainty $U(\bar{\rho})$, kg·m ⁻³	relative expanded uncertainty $U(\bar{\rho})/\bar{\rho}$, %
10	883.584	0.054	883.638	0.032	17	2.1075	0.067	0.0076
15	879.920	0.060	879.980	0.032	16	2.1195	0.067	0.0076
20	876.264	0.065	876.328	0.033	15	2.1205	0.069	0.0079
25	872.616	0.066	872.682	0.032	15	2.1221	0.069	0.0079
30	868.973	0.067	869.040	0.033	15	2.1233	0.071	0.0082
35	865.334	0.067	865.401	0.033	15	2.1230	0.071	0.0082
40	861.698	0.069	861.767	0.034	14	2.1361	0.074	0.0085
45	858.065	0.067	858.132	0.034	14	2.1367	0.074	0.0086
50	854.433	0.068	854.500	0.035	14	2.1365	0.076	0.0089

Table 1. continued

NIST SRM 2773 B100 biodiesel (animal fat-based)								
temp. t , °C	avg density $\bar{\rho}$, kg·m ⁻³	toluene correction C , kg·m ⁻³	corrected density $\bar{\rho}$, kg·m ⁻³	combined standard uncertainty $u(\bar{\rho})$, kg·m ⁻³	effective degrees of freedom df	coverage factor k at 95% uncertainty	expanded uncertainty $U(\bar{\rho})$, kg·m ⁻³	relative expanded uncertainty $U(\bar{\rho})/\bar{\rho}$, %
55	850.802	0.066	850.869	0.035	14	2.1384	0.076	0.0089
60	847.174	0.061	847.236	0.036	13	2.1540	0.078	0.0092
65	843.546	0.056	843.602	0.037	13	2.1543	0.080	0.0095
70	839.915	0.049	839.964	0.037	13	2.1548	0.080	0.0096

Table 2. Densities of Certified Biofuel Reference Materials and Their Uncertainties, as Measured with the Vibrating-Tube Densimeter 2 at Ambient Atmospheric Pressure (0.083 MPa)

AEAC anhydrous bioethanol							
temp. t , °C	avg density $\bar{\rho}$, kg·m ⁻³	combined standard uncertainty $u(\bar{\rho})$, kg·m ⁻³	effective degrees of freedom df	coverage factor k at 95% uncertainty	expanded uncertainty $U(\bar{\rho})$, kg·m ⁻³	relative expanded uncertainty $U(\bar{\rho})/\bar{\rho}$, %	
-10	815.62	0.12	28	2.046	0.24	0.029	
-5	811.36	0.10	32	2.035	0.21	0.026	
0	807.18	0.11	33	2.032	0.22	0.027	
5	802.88	0.10	32	2.037	0.21	0.026	
10	798.66	0.10	32	2.035	0.21	0.026	
15	794.36	0.10	32	2.035	0.21	0.026	
20	790.06	0.10	32	2.035	0.21	0.027	
25	785.76	0.10	32	2.035	0.21	0.027	
30	781.40	0.11	33	2.034	0.22	0.029	
35	777.02	0.11	33	2.032	0.22	0.028	
40	772.62	0.11	33	2.032	0.22	0.028	
45	768.14	0.11	31	2.038	0.23	0.030	
50	763.66	0.12	24	2.061	0.25	0.033	
55	759.10	0.12	23	2.066	0.25	0.033	
60	754.46	0.15	11	2.195	0.34	0.045	
AEHC hydrated bioethanol							
temp. t , °C	avg density $\bar{\rho}$, kg·m ⁻³	combined standard uncertainty $u(\bar{\rho})$, kg·m ⁻³	effective degrees of freedom df	coverage factor k at 95% uncertainty	expanded uncertainty $U(\bar{\rho})$, kg·m ⁻³	relative expanded uncertainty $U(\bar{\rho})/\bar{\rho}$, %	
-10	836.36	0.11	33	2.033	0.22	0.026	
-5	832.16	0.11	33	2.033	0.22	0.026	
0	828.02	0.11	32	2.036	0.23	0.027	
5	823.78	0.11	33	2.032	0.22	0.026	
10	819.46	0.11	33	2.033	0.22	0.027	
15	815.18	0.11	33	2.032	0.22	0.027	
20	810.84	0.11	31	2.038	0.23	0.028	
25	806.28	0.22	6	2.425	0.54	0.067	
30	801.64	0.36	4	2.625	0.96	0.119	
35	797.04	0.30	5	2.566	0.78	0.097	
40	792.66	0.23	5	2.451	0.57	0.072	
45	788.32	0.16	9	2.232	0.36	0.046	
50	783.84	0.12	21	2.075	0.26	0.033	
55	779.22	0.12	22	2.072	0.26	0.033	
60	774.50	0.13	18	2.097	0.27	0.035	
NIST SRM 2772 B100 Biodiesel (soy-based)							
temp. t , °C	avg density $\bar{\rho}$, kg·m ⁻³	combined standard uncertainty $u(\bar{\rho})$, kg·m ⁻³	effective degrees of freedom df	coverage factor k at 95% uncertainty	expanded uncertainty $U(\bar{\rho})$, kg·m ⁻³	relative expanded uncertainty $U(\bar{\rho})/\bar{\rho}$, %	
10	888.62	0.10	32	2.037	0.21	0.023	
15	884.96	0.10	32	2.035	0.21	0.024	
20	881.34	0.10	32	2.035	0.21	0.024	
25	877.60	0.10	30	2.042	0.20	0.023	
30	874.02	0.10	32	2.037	0.21	0.024	
35	870.40	0.10	30	2.042	0.20	0.023	
40	866.72	0.10	32	2.037	0.21	0.024	
45	863.02	0.10	32	2.037	0.21	0.024	
50	859.40	0.10	30	2.042	0.20	0.024	
55	855.78	0.10	32	2.037	0.21	0.024	
60	852.12	0.10	32	2.037	0.21	0.024	
65	848.50	0.10	30	2.042	0.20	0.024	

Table 2. continued

NIST SRM 2772 B100 Biodiesel (soy-based)						
temp. t , °C	avg density $\bar{\rho}$, kg·m ⁻³	combined standard uncertainty $u(\bar{\rho})$, kg·m ⁻³	effective degrees of freedom df	coverage factor k at 95% uncertainty	expanded uncertainty $U(\bar{\rho})$, kg·m ⁻³	relative expanded uncertainty $U(\bar{\rho})/\bar{\rho}$, %
70	844.88	0.10	32	2.037	0.21	0.025
75	841.22	0.10	32	2.037	0.21	0.025
80	837.62	0.10	32	2.037	0.21	0.025
85	834.00	0.10	30	2.042	0.20	0.024
90	830.34	0.10	32	2.035	0.21	0.025
95	826.70	0.10	30	2.042	0.20	0.025
100	823.10	0.10	30	2.042	0.20	0.025
NIST SRM 2773 B100 Biodiesel (animal fat-based)						
temp. t , °C	avg density $\bar{\rho}$, kg·m ⁻³	combined standard uncertainty $u(\bar{\rho})$, kg·m ⁻³	effective degrees of freedom df	coverage factor k at 95% uncertainty	expanded uncertainty $U(\bar{\rho})$, kg·m ⁻³	relative expanded uncertainty $U(\bar{\rho})/\bar{\rho}$, %
10	883.58	0.10	32	2.037	0.21	0.024
15	879.88	0.10	32	2.037	0.21	0.024
20	876.22	0.10	32	2.037	0.21	0.024
25	872.56	0.10	32	2.035	0.21	0.024
30	868.90	0.10	30	2.042	0.20	0.024
35	865.26	0.10	32	2.035	0.21	0.024
40	861.62	0.10	32	2.037	0.21	0.024
45	857.96	0.10	32	2.035	0.21	0.024
50	854.32	0.10	32	2.037	0.21	0.024
55	850.72	0.10	32	2.037	0.21	0.024
60	847.08	0.11	33	2.032	0.22	0.026
65	843.44	0.10	32	2.035	0.21	0.025
70	839.80	0.10	30	2.042	0.20	0.024
75	836.18	0.10	32	2.037	0.21	0.025
80	832.56	0.10	32	2.035	0.21	0.025
85	828.92	0.10	32	2.037	0.21	0.025
90	825.28	0.10	32	2.037	0.21	0.025
95	821.64	0.10	32	2.035	0.21	0.025
100	818.02	0.11	33	2.032	0.22	0.027

Table 3. Speeds of Sound of Certified Biofuel Reference Materials and Their Uncertainties, as Measured with the Sound Speed Analyzer at Ambient Atmospheric Pressure (0.083 MPa)

AEAC anhydrous bioethanol						
temp. t , °C	avg speed of sound \bar{w} , m·s ⁻¹	combined standard uncertainty $u(\bar{w})$, m·s ⁻¹	effective degrees of freedom df	coverage factor k at 95% uncertainty	expanded uncertainty $U(\bar{w})$, m·s ⁻¹	relative expanded uncertainty $U(\bar{w})/\bar{w}$, %
5	1217.26	0.33	3	2.8927	0.96	0.079
10	1199.48	0.31	3	2.8628	0.90	0.075
15	1181.86	0.30	3	2.8410	0.86	0.072
20	1164.43	0.28	3	2.7918	0.78	0.067
25	1147.15	0.26	4	2.7350	0.70	0.061
30	1130.04	0.25	4	2.7192	0.68	0.060
35	1113.06	0.23	4	2.6611	0.62	0.056
40	1096.14	0.20	5	2.5390	0.51	0.047
45	1079.25	0.16	7	2.3345	0.38	0.035
50	1062.50	0.15	9	2.2299	0.32	0.031
55	1045.77	0.10	32	2.0352	0.21	0.020
60	1029.24	0.11	27	2.0494	0.23	0.022
AEHC hydrated bioethanol						
temp. t , °C	avg speed of sound \bar{w} , m·s ⁻¹	combined standard uncertainty $u(\bar{w})$, m·s ⁻¹	effective degrees of freedom df	coverage factor k at 95% uncertainty	expanded uncertainty $U(\bar{w})$, m·s ⁻¹	relative expanded uncertainty $U(\bar{w})/\bar{w}$, %
5	1273.94	0.12	25	2.0581	0.25	0.019
10	1256.47	0.12	28	2.0458	0.24	0.019
15	1239.08	0.12	25	2.0573	0.25	0.020
20	1221.80	0.12	26	2.0539	0.24	0.020
25	1204.60	0.12	27	2.0501	0.24	0.020
30	1187.46	0.12	28	2.0474	0.24	0.020
35	1170.36	0.11	30	2.0415	0.23	0.020
40	1153.26	0.11	31	2.0391	0.23	0.020
45	1136.22	0.11	31	2.0393	0.23	0.020

Table 3. continued

AEHC hydrated bioethanol						
temp. t , °C	avg speed of sound \bar{w} , m·s ⁻¹	combined standard uncertainty $u(\bar{w})$, m·s ⁻¹	effective degrees of freedom df	coverage factor k at 95% uncertainty	expanded uncertainty $U(\bar{w})$, m·s ⁻¹	relative expanded uncertainty $U(\bar{w})/\bar{w}$, %
50	1119.17	0.12	29	2.0447	0.24	0.021
55	1102.09	0.12	25	2.0578	0.25	0.022
60	1085.07	0.11	30	2.0422	0.23	0.022
NIST SRM 2772 B100 biodiesel (soy-based)						
temp. t , °C	avg speed of sound \bar{w} , m·s ⁻¹	combined standard uncertainty $u(\bar{w})$, m·s ⁻¹	effective degrees of freedom df	coverage factor k at 95% uncertainty	expanded uncertainty $U(\bar{w})$, m·s ⁻¹	relative expanded uncertainty $U(\bar{w})/\bar{w}$, %
5	1467.81	0.14	15	2.1216	0.29	0.020
10	1449.21	0.14	14	2.1317	0.30	0.020
15	1430.79	0.14	14	2.1405	0.30	0.021
20	1412.58	0.14	14	2.1378	0.30	0.021
25	1394.56	0.14	13	2.1548	0.31	0.022
30	1376.74	0.14	13	2.1578	0.31	0.023
35	1359.08	0.15	12	2.1787	0.33	0.024
40	1341.58	0.15	11	2.1917	0.33	0.025
45	1324.25	0.16	10	2.2187	0.35	0.027
50	1307.09	0.17	9	2.2586	0.38	0.029
55	1290.07	0.17	8	2.2775	0.40	0.031
60	1273.21	0.19	7	2.3289	0.44	0.035
65	1256.56	0.20	6	2.3778	0.49	0.039
70	1240.12	0.21	6	2.3918	0.50	0.040
NIST SRM 2773 B100 biodiesel (animal fat-based)						
temp. t , °C	avg speed of sound \bar{w} , m·s ⁻¹	combined standard uncertainty $u(\bar{w})$, m·s ⁻¹	effective degrees of freedom df	coverage factor k at 95% uncertainty	expanded uncertainty $U(\bar{w})$, m·s ⁻¹	relative expanded uncertainty $U(\bar{w})/\bar{w}$, %
10	1444.60	0.18	8	2.3050	0.42	0.029
15	1426.11	0.19	7	2.3186	0.43	0.030
20	1407.83	0.18	7	2.3145	0.43	0.030
25	1389.70	0.18	7	2.3118	0.42	0.031
30	1371.80	0.19	7	2.3175	0.43	0.031
35	1354.10	0.20	7	2.3496	0.46	0.034
40	1336.56	0.20	6	2.3667	0.48	0.036
45	1319.17	0.21	6	2.4027	0.51	0.039
50	1301.99	0.23	5	2.4489	0.57	0.044
55	1284.99	0.26	5	2.4980	0.64	0.050
60	1268.11	0.27	5	2.5233	0.69	0.054
65	1251.40	0.28	5	2.5413	0.72	0.058
70	1234.79	0.24	5	2.4632	0.59	0.048

Table 4. Viscosities of Certified Biofuel Reference Materials and Their Uncertainties, as Measured with the Open Gravitational Capillary Viscometer (Viscometer 1) at Ambient Atmospheric Pressure (0.083 MPa)

AEAC anhydrous bioethanol							
temp. t , °C	avg efflux time $\bar{\tau}$, s	avg adjusted kinematic viscosity, mm ² ·s ⁻¹	combined standard uncertainty $u(\bar{\nu})$, mm ² ·s ⁻¹	effective degrees of freedom df	coverage factor k at 95% uncertainty	expanded uncertainty $U(\bar{\nu})$, mm ² ·s ⁻¹	relative expanded uncertainty $U(\bar{\nu})/\bar{\nu}$, %
20	145.40	1.527	0.0012	24	2.0639	0.0025	0.16
25	132.81	1.394	0.0010	50	2.0086	0.0021	0.15
30	121.71	1.276	0.0010	55	2.0040	0.0020	0.16
35	111.57	1.169	0.0010	55	2.0040	0.0020	0.17
40	102.78	1.075	0.0010	53	2.0058	0.0021	0.20
45	94.747	0.9899	0.0011	49	2.0096	0.0023	0.23
50	87.663	0.9143	0.0012	41	2.0195	0.0024	0.26
55	81.277	0.8458	0.0013	37	2.0262	0.0026	0.31
60	75.487	0.7834	0.0014	32	2.0369	0.0029	0.37
AEHC hydrated bioethanol							
temp. t , °C	avg efflux time $\bar{\tau}$, s	avg adjusted kinematic viscosity, mm ² ·s ⁻¹	combined standard uncertainty $u(\bar{\nu})$, mm ² ·s ⁻¹	effective degrees of freedom df	coverage factor k at 95% uncertainty	expanded uncertainty $U(\bar{\nu})$, mm ² ·s ⁻¹	relative expanded uncertainty $U(\bar{\nu})/\bar{\nu}$, %
20	177.91	1.870	0.0029	14	2.1448	0.0062	0.33
25	159.07	1.671	0.0019	20	2.0860	0.0039	0.23

Table 4. continued

AEHC hydrated bioethanol							
temp. t , °C	avg efflux time $\bar{\tau}$, s	avg adjusted kinematic viscosity, mm^2s^{-1}	combined standard uncertainty $u(\bar{\nu})$, mm^2s^{-1}	effective degrees of freedom df	coverage factor k at 95% uncertainty	expanded uncertainty $U(\bar{\nu})$, mm^2s^{-1}	relative expanded uncertainty $U(\bar{\nu})/\bar{\nu}$, %
30	143.11	1.503	0.0017	11	2.2010	0.0037	0.24
35	129.08	1.354	0.0013	52	2.0067	0.0026	0.19
40	117.30	1.230	0.0012	51	2.0076	0.0025	0.20
45	107.02	1.120	0.0012	53	2.0058	0.0024	0.22
50	97.720	1.022	0.0012	52	2.0067	0.0025	0.24
55	89.743	0.9365	0.0013	53	2.0058	0.0026	0.28
60	82.630	0.8603	0.0014	48	2.0106	0.0029	0.33
NIST SRM 2772 B100 biodiesel (soy-based)							
temp. t , °C	avg efflux time $\bar{\tau}$, s	avg adjusted kinematic viscosity, mm^2s^{-1}	combined standard uncertainty $u(\bar{\nu})$, mm^2s^{-1}	effective degrees of freedom df	coverage factor k at 95% uncertainty	expanded uncertainty $U(\bar{\nu})$, mm^2s^{-1}	relative expanded uncertainty $U(\bar{\nu})/\bar{\nu}$, %
20	74.747	6.429	0.0068	30	2.0423	0.014	0.22
25	66.000	5.675	0.0064	8	2.3060	0.015	0.26
30	58.797	5.053	0.0047	35	2.0301	0.0095	0.19
35	52.617	4.519	0.0050	31	2.0395	0.010	0.22
40	47.503	4.077	0.0050	35	2.0301	0.010	0.25
45	43.127	3.698	0.0058	23	2.0687	0.012	0.33
50	39.273	3.363	0.0063	17	2.1098	0.013	0.39
55	36.000	3.078	0.0070	12	2.1788	0.015	0.50
60	270.57	2.846	0.0044	25	2.0595	0.0090	0.32
65	249.96	2.629	0.0038	28	2.0484	0.0077	0.29
70	231.83	2.438	0.0033	35	2.0301	0.0067	0.28
75	216.23	2.273	0.0030	39	2.0227	0.0060	0.26
80	202.08	2.124	0.0027	40	2.0211	0.0054	0.26
85	189.34	1.990	0.0026	41	2.0195	0.0052	0.26
90	177.85	1.869	0.0024	40	2.0211	0.0049	0.26
95	167.57	1.761	0.0024	37	2.0262	0.0049	0.28
100	158.25	1.662	0.0024	34	2.0322	0.0049	0.30
NIST SRM 2773 B100 Biodiesel (animal fat-based)							
temp. t , °C	avg efflux time $\bar{\tau}$, s	avg adjusted kinematic viscosity, mm^2s^{-1}	combined standard uncertainty $u(\bar{\nu})$, mm^2s^{-1}	effective degrees of freedom df	coverage factor k at 95% uncertainty	expanded uncertainty $U(\bar{\nu})$, mm^2s^{-1}	relative expanded uncertainty $U(\bar{\nu})/\bar{\nu}$, %
20	83.293	7.166	0.0071	47	2.0117	0.014	0.20
25	72.860	6.266	0.0060	33	2.0345	0.012	0.20
30	64.517	5.547	0.0059	17	2.1098	0.013	0.23
35	57.493	4.941	0.0052	37	2.0262	0.011	0.21
40	421.03	4.429	0.0045	43	2.0167	0.0090	0.20
45	380.18	3.999	0.0041	40	2.0211	0.0083	0.21
50	345.20	3.631	0.0038	39	2.0227	0.0078	0.21
55	315.10	3.314	0.0036	37	2.0262	0.0073	0.22
60	288.92	3.039	0.0034	36	2.0281	0.0069	0.23
65	266.09	2.798	0.0032	36	2.0281	0.0064	0.23
70	245.97	2.587	0.0030	35	2.0301	0.0060	0.23
75	228.32	2.401	0.0028	33	2.0345	0.0057	0.24
80	212.62	2.235	0.0026	33	2.0345	0.0054	0.24
85	198.59	2.088	0.0025	33	2.0345	0.0051	0.24
90	186.07	1.956	0.0024	34	2.0322	0.0048	0.25
95	174.84	1.837	0.0023	34	2.0322	0.0046	0.25
100	164.67	1.730	0.0022	35	2.0301	0.0044	0.26

Table 5. Viscosities of Certified Biofuel Reference Materials and Their Uncertainties, as Measured with the Rotating Concentric Cylinder Viscometer (Viscometer 2) at Ambient Atmospheric Pressure (0.083 MPa)

AEAC anhydrous bioethanol						
temp. t , °C	avg dynamic viscosity $\bar{\eta}$, mPa·s	combined standard uncertainty $u(\bar{\eta})$, mPa·s	effective degrees of freedom df	coverage factor k at 95% uncertainty	expanded uncertainty $U(\bar{\eta})$, mPa·s	relative expanded uncertainty $U(\bar{\eta})/\bar{\eta}$, %
-10	2.226	0.0019	92	1.9861	0.0038	0.17
-5	1.997	0.0016	76	1.9917	0.0032	0.16
0	1.796	0.0014	72	1.9935	0.0028	0.15

Table 5. continued

AEAC anhydrous bioethanol						
temp. t , °C	avg dynamic viscosity $\bar{\eta}$, mPa·s	combined standard uncertainty $u(\bar{\eta})$, mPa·s	effective degrees of freedom df	coverage factor k at 95% uncertainty	expanded uncertainty $U(\bar{\eta})$, mPa·s	relative expanded uncertainty $U(\bar{\eta})/\bar{\eta}$, %
5	1.619	0.0013	75	1.9921	0.0025	0.15
10	1.464	0.0011	78	1.9909	0.0023	0.16
15	1.327	0.0010	81	1.9897	0.0021	0.16
20	1.205	0.0010	82	1.9893	0.0019	0.16
25	1.097	0.0009	82	1.9893	0.0017	0.16
30	1.000	0.0008	82	1.9893	0.0016	0.16
35	0.9139	0.0007	85	1.9883	0.0015	0.16
40	0.8363	0.0008	41	2.0195	0.0016	0.19
45	0.7658	0.0011	9	2.2622	0.0026	0.34
50	0.7015	0.0018	5	2.5706	0.0047	0.67
55	0.6419	0.0024	4	2.7765	0.0068	1.05
60	0.5876	0.0029	4	2.7765	0.0082	1.39
AEHC hydrated bioethanol						
temp. t , °C	avg dynamic viscosity $\bar{\eta}$, mPa·s	combined standard uncertainty $u(\bar{\eta})$, mPa·s	effective degrees of freedom df	coverage factor k at 95% uncertainty	expanded uncertainty $U(\bar{\eta})$, mPa·s	relative expanded uncertainty $U(\bar{\eta})/\bar{\eta}$, %
-10	3.280	0.0036	25	2.0595	0.0075	0.23
-5	2.848	0.0029	30	2.0423	0.0058	0.21
0	2.486	0.0025	26	2.0555	0.0052	0.21
5	2.181	0.0020	51	2.0076	0.0039	0.18
10	1.924	0.0017	64	1.9977	0.0033	0.17
15	1.704	0.0015	70	1.9944	0.0029	0.17
20	1.516	0.0012	78	1.9909	0.0025	0.16
25	1.355	0.0011	75	1.9921	0.0022	0.16
30	1.215	0.0010	78	1.9909	0.0020	0.16
35	1.093	0.0009	77	1.9913	0.0018	0.17
40	0.9863	0.0009	68	1.9955	0.0017	0.18
45	0.8920	0.0009	39	2.0227	0.0018	0.20
50	0.8075	0.0010	22	2.0739	0.0020	0.25
55	0.7310	0.0010	20	2.0860	0.0020	0.28
60	0.6609	0.0016	6	2.4469	0.0040	0.60
NIST SRM 2772 B100 Biodiesel (soy-based)						
temp. t , °C	avg dynamic viscosity $\bar{\eta}$, mPa·s	combined standard uncertainty $u(\bar{\eta})$, mPa·s	effective degrees of freedom df	coverage factor k at 95% uncertainty	expanded uncertainty $U(\bar{\eta})$, mPa·s	relative expanded uncertainty $U(\bar{\eta})/\bar{\eta}$, %
10	7.548	0.0124	8	2.3060	0.029	0.38
15	6.512	0.0098	8	2.3060	0.023	0.35
20	5.674	0.0070	12	2.1788	0.015	0.27
25	4.988	0.0066	10	2.2281	0.015	0.29
30	4.420	0.0055	11	2.2010	0.012	0.28
35	3.945	0.0047	13	2.1604	0.010	0.26
40	3.545	0.0040	15	2.1315	0.0085	0.24
45	3.204	0.0034	18	2.1009	0.0072	0.22
50	2.912	0.0030	21	2.0796	0.0062	0.21
55	2.659	0.0026	25	2.0595	0.0054	0.20
60	2.439	0.0023	29	2.0452	0.0048	0.20
65	2.246	0.0021	39	2.0227	0.0043	0.19
70	2.076	0.0019	52	2.0067	0.0039	0.19
75	1.925	0.0018	71	1.9939	0.0037	0.19
80	1.791	0.0018	96	1.9850	0.0035	0.20
85	1.670	0.0017	119	1.9801	0.0034	0.21
90	1.561	0.0017	130	1.9784	0.0035	0.22
95	1.462	0.0018	134	1.9778	0.0035	0.24
100	1.372	0.0018	132	1.9781	0.0036	0.26
NIST SRM 2773 B100 biodiesel (animal fat-based)						
temp. t , °C	avg dynamic viscosity $\bar{\eta}$, mPa·s	combined standard uncertainty $u(\bar{\eta})$, mPa·s	effective degrees of freedom df	coverage factor k at 95% uncertainty	expanded uncertainty $U(\bar{\eta})$, mPa·s	relative expanded uncertainty $U(\bar{\eta})/\bar{\eta}$, %
10	8.489	0.0079	69	1.9950	0.016	0.19
15	7.262	0.0064	66	1.9966	0.013	0.18
20	6.278	0.0053	66	1.9966	0.011	0.17

Table 5. continued

NIST SRM 2773 B100 biodiesel (animal fat-based)						
temp. t , °C	avg dynamic viscosity $\bar{\eta}$, mPa·s	combined standard uncertainty $u(\bar{\eta})$, mPa·s	effective degrees of freedom df	coverage factor k at 95% uncertainty	expanded uncertainty $U(\bar{\eta})$, mPa·s	relative expanded uncertainty $U(\bar{\eta})/\bar{\eta}$, %
25	5.480	0.0045	67	1.9960	0.0090	0.16
30	4.824	0.0038	68	1.9955	0.0077	0.16
35	4.279	0.0033	68	1.9955	0.0067	0.16
40	3.823	0.0029	67	1.9960	0.0058	0.15
45	3.438	0.0026	66	1.9966	0.0052	0.15
50	3.109	0.0023	64	1.9977	0.0046	0.15
55	2.827	0.0021	63	1.9983	0.0041	0.15
60	2.582	0.0019	63	1.9983	0.0037	0.14
65	2.369	0.0017	63	1.9983	0.0034	0.14
70	2.182	0.0016	66	1.9966	0.0032	0.14
75	2.017	0.0015	70	1.9944	0.0030	0.15
80	1.870	0.0014	77	1.9913	0.0028	0.15
85	1.739	0.0014	85	1.9883	0.0027	0.15
90	1.622	0.0013	95	1.9853	0.0026	0.16
95	1.516	0.0013	105	1.9828	0.0026	0.17
100	1.419	0.0013	117	1.9805	0.0025	0.18

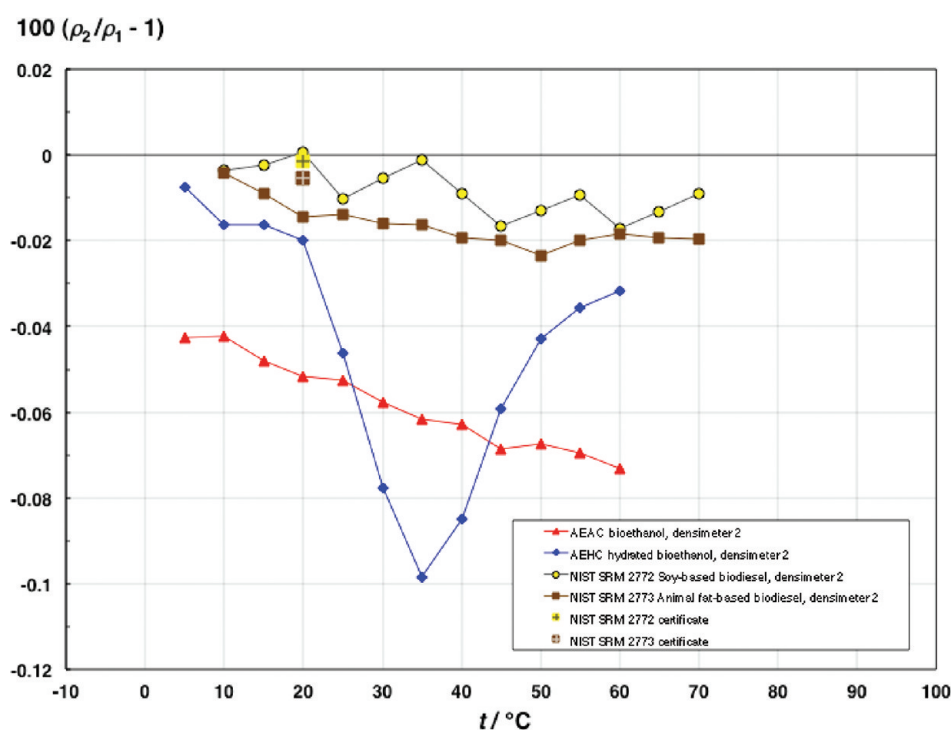


Figure 9. Relative deviations of densities from those measured in densimeter 1 as a function of temperature.

same sequence as the densities from AEAC to AEHC to NIST SRM 2773 and NIST SRM 2772. However, the temperature dependencies appear linear and parallel for all four samples.

3.3. Viscosity Measurements. The results of the viscosity measurements of the four sample liquids are listed in Table 4 for viscometer 1 and in Table 5 for viscometer 2. Included in the tables are the estimated uncertainties, which have been calculated as described in Appendix A3 of the Supporting Information for the open gravitational capillary viscometer and in Appendix A4 of the Supporting Information for the rotating concentric cylinder viscometer. Figure 11 displays the kinematic viscosities of all four samples as a function of temperature. It is noteworthy that the viscosity of the animal fat-based biodiesel NIST SRM 2773 is higher than that of the soy-based NIST SRM 2772, whereas the densities and speeds of sound of the

two samples are reversed. This difference between viscosity on one hand and density and speed of sound on the other is important for practitioners in the biofuels industry. The viscosities of the bioethanol samples increase in the same order as their densities and speeds of sound, with that of AEHC hydrated bioethanol being higher than that of AEAC anhydrous bioethanol. Again, this dependence is consistent with the well-known viscosity–composition dependence in water–ethanol mixtures.^{29,30}

Relative deviations of the viscosities measured with viscometer 2 from those measured with viscometer 1 are shown in Figures 12 and 13 as a function of temperature. At 20 °C, all results of the two instruments for the four samples agree within 0.2% and within their respective calculated expanded uncertainties. Systematic deviations that exceed the calculated

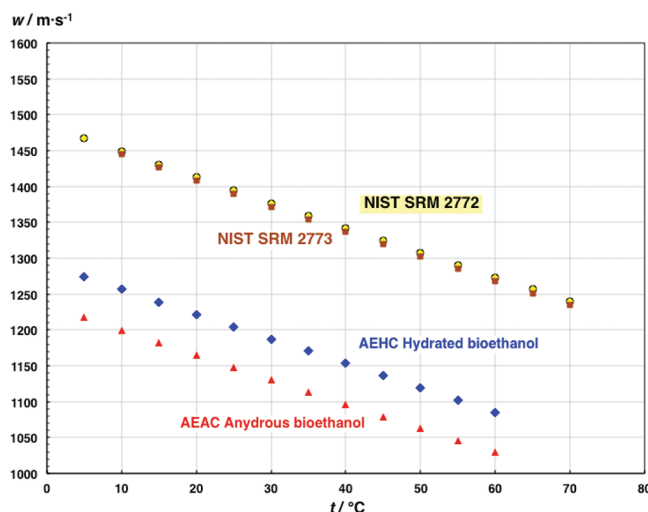


Figure 10. Measured speed of sound data of biofuel reference materials as a function of temperature.

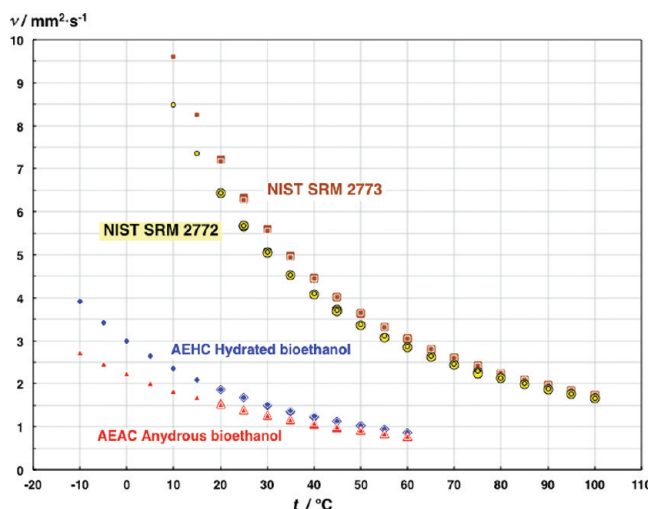


Figure 11. Measured kinematic viscosities of biofuel reference materials as a function of temperature. Large symbols denote data measured with viscometer 1. Small symbols denote data measured with viscometer 2.

expanded uncertainties are observed at the higher temperatures. The deviations for the bioethanol samples AEAC and AEHC increase to maxima of 0.71% at 45 °C and 1.15% at 35 °C, respectively, before they decrease to -0.58% and -0.85% at 60 °C. The deviations at 60 °C are again within the calculated expanded uncertainties of the results of viscometer 2 for these samples.

The deviations between the measured viscosities of the biodiesel samples are systematically positive at all temperatures. The results from viscometer 2 for NIST SRM 2772 deviate at a maximum of 0.94% at 55 °C and decrease to 0.30% at 100 °C. It is noteworthy that the viscosities that are currently on the certificate of NIST SRM 2772⁷ at 20 °C, 30 °C, and 40 °C deviate from the results of viscometer 1 by only 0.03%, 0.0%, and 0.18%, respectively. These deviations are within the calculated expanded uncertainty of the results of viscometer 1. The certificate viscosities are a statistical combination of measurements at Cannon Instrument Comp., at Inmetro, and of those with viscometer 2.

Figure 13 displays the corresponding deviations for NIST SRM 2773. The results from viscometer 2 for NIST SRM 2773 deviate at most 0.52% at 80 °C and decrease to 0.30% at 100 °C. Again, it is noteworthy that the viscosities that are currently on

the certificate of NIST SRM 2773⁸ at 20 °C, 30 °C, and 40 °C deviate from the results of viscometer 1 by only -0.27% , 0.07%, and 0.02%, respectively. Except at 20 °C, these deviations are within the calculated expanded uncertainty of the results of viscometer 1. The certificate viscosities are a statistical combination of measurements at Cannon Instrument Comp., at Inmetro, and of those with viscometer 2.

4. CONCLUDING REMARKS

Four reference materials for the biofuel industry were characterized in this work with respect to their density, speed of sound, and viscosity. The importance of accurate density and viscosity data for the fuels industry is self-evident. The speed of sound is also of practical relevance because it characterizes the compressibility of fuels, which is of interest for internal combustion engines and injection systems. There is also growing scientific interest in the speed of sound for the development of thermodynamic property formulations. The growing interest is met by more readily available instrumentation to measure this property, and this in turn requires measurement standards and reference materials. This work is a contribution that addresses this emerging need.

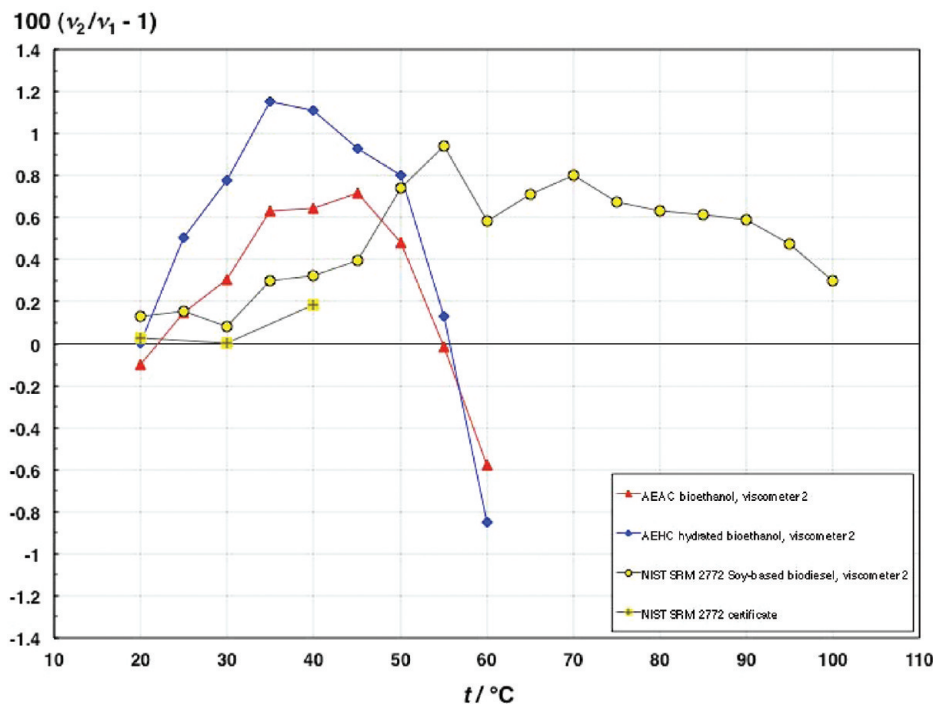


Figure 12. Relative deviations of viscosities of the bioethanol materials and NIST SRM 2772 biodiesel from those measured with viscometer 1 as a function of temperature.

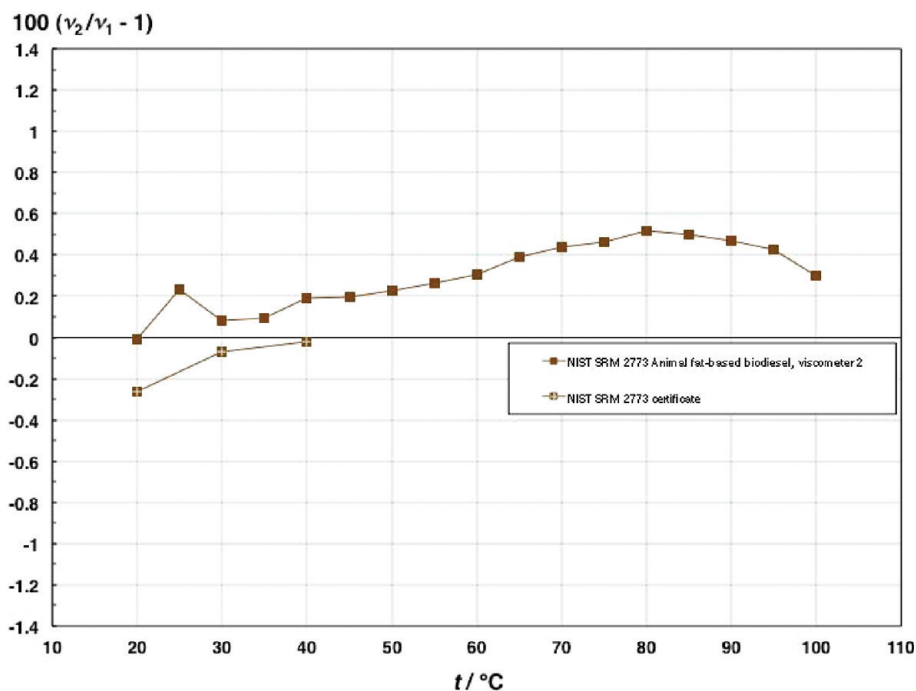


Figure 13. Relative deviations of viscosities of NIST SRM 2773 biodiesel from those measured with viscometer 1 as a function of temperature.

The four reference materials were anhydrous and hydrated bioethanol and the NIST B100 Biodiesel Standard Reference Materials 2772 (soy-based) and 2773 (animal fat-based). Their properties were measured at ambient pressure and over extended temperature ranges. Primary density and speed of sound data are reported in the range 5 to 60 °C for the bioethanol samples and in the range 10 to 70 °C for the biodiesel samples. Supplementary density data range to -10 °C for the bioethanol samples and to 100 °C for the biodiesel

samples. Primary viscosity data are reported in the range 20 to 60 °C for the bioethanol samples and to 100 °C for the biodiesel samples. Supplementary viscosity data range to -10 °C for the bioethanol samples and to 10 °C for the biodiesel samples. Extended range reference data provide a broader foundation for the calibration of industrial instruments. Extended range reference data are especially valuable for the viscosity, because the temperature dependence of the viscosity is as important as the viscosity itself.

The measurement results are reported with detailed uncertainty analyses to promote such assessments as integral parts of sound metrology.

Besides the provision of reference data, this work has also reference character with regard to the measurement methods and protocols that were practiced. Density and viscosity were measured in two instruments for each property. While both densimeters had vibrating-tube sensors, the viscometers were based on gravitational flow through a vertical capillary and on sensing the shear between rotating concentric cylinders according to Stabinger. The results of this work provide valuable comparisons of the performance of these instruments. All three instruments are widely used in scientific and industrial laboratories. Thus, the methods and procedures that were employed in this work are of immediate applicability for quality assurance in many other laboratories. It is hoped that this work will contribute to the development of standards and test methods for thermophysical properties measurements by standards organizations.

■ ASSOCIATED CONTENT

● Supporting Information

Detailed descriptions of the uncertainty calculations for each of the four instruments. This information is available free of charge via the Internet at <http://pubs.acs.org/>.

■ AUTHOR INFORMATION

Corresponding Author

*Phone: 1-303-497-3197. Fax: 1-303-497-5224. E-mail: Arno.Laesecke@Boulder.NIST.Gov.

Notes

The authors declare no competing financial interest.

■ ACKNOWLEDGMENTS

Dr. Michele Schantz (NIST Gaithersburg, Analytical Chemistry Division) provided the samples and reviewed the manuscript. Dr. Mark McLinden and Stephanie Outcalt in the NIST Thermophysical Properties Division are acknowledged for many fruitful discussions. Dr. Wolfgang Belitsch (Labor für Messtechnik Dr. Hans Stabinger, Graz, Austria) provided details of the Stabinger viscometer, and Darren Wilson (Anton Paar USA, Ashland, Virginia) provided instrument support on many occasions. We acknowledge Pat Maggi, Tom Zubler, and Dan Novacco (Cannon Instrument Company, State College, Pennsylvania) for cooperation with certified viscosity standards and with the capillary viscometer. Arno Laesecke also thanks Dr. Scott Bair of the Center for High Pressure Rheology at the Georgia Institute of Technology (Atlanta, Georgia) for insightful discussions. The careful reading of an anonymous journal reviewer helped to improve the manuscript.

■ REFERENCES

- (1) Knothe, G. Biodiesel and Renewable Diesel: A Comparison. *Prog. Energy Combust. Sci.* **2010**, *36*, 364–373.
- (2) Smith, P. C.; Ngothai, Y.; Dzuy Nguyen, Q.; O'Neill, B. K. Improving the Low-Temperature Properties of Biodiesel: Methods and Consequences. *Renew. Energy* **2010**, *35*, 1145–1151.
- (3) Charlet, P.; Sommer, K.-D.; Filtz, J.-R.; Bauer, H. *BioFuels Met 2008, Biofuels and Metrology*, Strasbourg, France, 6-7 Nov 2008. Available online: https://www.ptb.de/cms/fileadmin/internet/fachabteilungen/abteilung_3/3.3_chemisch_physikalische_stoffeigenschaften/BioFuels_Mappe_2.pdf.

- (4) Barbosa, A. P. F.; Rodrigues, C. R. d. C.; Santo Filho, D. M. d. E.; Siqueira, J. R.; Pereira, R. G.; de Oliveira, L. H. P. Metrological Approach in the Characterization of Viscosity of Corn Biodiesel Relative to Temperature, Using Capillary Viscometers. *XIX IMEKO World Congress Fundamental and Applied Metrology Lisbon, Portugal*, 2009, p 1199–1202.

- (5) Santo Filho, D.; Pereira, R.; Rodrigues, C.; Barbosa, A. The Possibility of Using Beef Tallow Biodiesel As a Viscosity Reference Material. *Accredit. Qual. Assur.* **2010**, *15*, 473–476.

- (6) McLinden, M. O.; Bruno, T. J.; Frenkel, M.; Huber, M. L. Standard Reference Data for the Thermophysical Properties of Biofuels. *J. ASTM Int.* **2010**, *7*, 1–18.

- (7) Wise, S. A.; Watters, R. L. *NIST Standard Reference Material 2772 B100 Biodiesel (Soy-Based) Certificate of Analysis*, National Institute of Standards and Technology: Gaithersburg, MD, 2009. Available online: https://www-s.nist.gov/srmors/view_cert.cfm?srm=2772.

- (8) Wise, S. A.; Watters, R. L. *NIST Standard Reference Material 2773 B100 Biodiesel (Animal-Based) Certificate of Analysis*, National Institute of Standards and Technology: Gaithersburg, MD, 2009. Available online: https://www-s.nist.gov/srmors/view_cert.cfm?srm=2773.

- (9) *International Vocabulary of Metrology—Basic and General Concepts and Associated Terms (VIM)*, Joint Committee for Guides in Metrology: France, 2008. Available online: <http://www.bipm.org/en/publications/guides/vim.html>.

- (10) McLinden, M. O.; Splett, J. D. A Liquid Density Standard Over Wide Ranges of Temperature and Pressure Based on Toluene. *J. Res. Natl. Inst. Stand. Technol.* **2008**, *113*, 29–67.

- (11) Wagner, W.; Pruß, A. The IAPWS Formulation 1995 for the Thermodynamic Properties of Ordinary Water Substance for General and Scientific Use. *J. Phys. Chem. Ref. Data* **2002**, *31*, 387–536.

- (12) Lemmon, E. W.; Penoncello, S. G.; Jacobsen, R. T.; Friend, D. G. Thermodynamic Properties of Air and Mixtures of Nitrogen, Argon, and Oxygen From 60 to 2000 K at Pressures to 2000 MPa. *J. Phys. Chem. Ref. Data* **2000**, *29*, 331–385.

- (13) Lemmon, E. W.; Huber, M. L.; McLinden, M. O.; *NIST Standard Reference Database 23: Reference Fluid Thermodynamic and Transport Properties*, REFPROP, Version 9.0; National Institute of Standards and Technology: Gaithersburg, MD, 2010. Available online: <http://www.nist.gov/srd/nist23.cfm>.

- (14) Meier, K.; Kabelac, S. Measurements of the Speed of Sound in Liquid Toluene in the Temperature Range between 240 and 420 K at Pressures up to 100 MPa; Personal communication 2006.

- (15) Meier, K.; Kabelac, S. Speed of Sound Instrument for Fluids with Pressures up to 100 MPa; *Rev. Sci. Instrum.* **2006**, *77*, 123903 (8 pages).

- (16) Lemmon, E. W.; Span, R. Short Fundamental Equations of State for 20 Industrial Fluids. *J. Chem. Eng. Data* **2006**, *51*, 785–850.

- (17) Laesecke, A.; Outcalt, S.; Brumback, K. Density and Speed of Sound Measurements of Methyl- and Propylcyclohexane. *Energy Fuels* **2008**, *22*, 2629–2636.

- (18) Ott, L. S.; Huber, M. L.; Bruno, T. J. Density and Speed of Sound Measurements on Five Fatty Acid Methyl Esters at 83 kPa and Temperatures from 278.15 to 338.15 K. *J. Chem. Eng. Data* **2008**, *53*, 2412–2416.

- (19) Outcalt, S.; Laesecke, A.; Freund, M. B. Density and Speed of Sound Measurements of Aviation Turbine Fuels. *Energy Fuels* **2009**, *23*, 1626–1633.

- (20) Outcalt, S. L.; Laesecke, A.; Brumback, K. J. Thermophysical Properties Measurements of Rocket Propellants RP-1 and RP-2. *J. Propul. Power* **2009**, *25*, 1032–1040.

- (21) Outcalt, S. L.; Laesecke, A.; Brumback, K. J. Comparison of Jet Fuels by Density and Speed of Sound Measurements of a Flightline JP-8. *Energy Fuels* **2010**, *24*, 5573–5578.

- (22) Outcalt, S. L.; Laesecke, A.; Fortin, T. J. Density and Speed of Sound Measurements of Hexadecane. *J. Chem. Thermodyn.* **2010**, *42*, 700–706.

- (23) Outcalt, S. L.; Laesecke, A.; Fortin, T. J. Density and Speed of Sound Measurements of 1- and 2-Butanol. *J. Mol. Liq.* **2010**, *151*, 50–59.

(24) Outcalt, S. L.; Laesecke, A. Measurements of Density and Speed of Sound of JP-10 and Comparison to Rocket Propellants and Jet Fuels. *Energy Fuels* **2011**, *25*, 1132–1139.

(25) Outcalt, S. L.; Fortin, T. J. Density and Speed of Sound Measurements of Two Synthetic Aviation Turbine Fuels. *J. Chem. Eng. Data* **2011**, *56*, 3201–3207.

(26) Kawata, M.; Kurase, K.; Nagashima, A.; Yoshida, K. *Measurement of the Transport Properties of Fluids*, 1st ed.; Wakeham, W. A., Nagashima, A., Sengers, J. V., Eds.; Blackwell Scientific Publications: Oxford, U.K., 1991; Vol. 3, pp 49–76.

(27) ASTM. *Standard Specifications and Operating Instructions for Glass Capillary Kinematic Viscometers*, ASTM D446-07; ASTM: West Conshohocken, PA, 2009. Available online: <http://www.astm.org/Standards/D446.htm>.

(28) Tanaka, Y.; Yamamoto, T.; Satomi, Y.; Kubota, H.; Makita, T. Specific Volume and Viscosity of Ethanol–Water Mixtures Under High Pressure. *Rev. Phys. Chem. Jpn.* **1977**, *47*, 12–24.

(29) Wohlfarth, C.; Wohlfarth, B. Viscosity of Pure Organic Liquids and Binary Liquid Mixtures, Subvolume A: Pure Organometallic and Organononmetallic Liquids and Binary Liquid Mixtures. In *Landolt–Börnstein—Numerical Data and Functional Relationships in Science and Technology*; Lechner, M. D., Ed.; Springer-Verlag: Berlin, Heidelberg, New York, 2001; Vol. IV/18.

(30) Wohlfarth, C. Viscosity of Pure Organic Liquids and Binary Liquid Mixtures. In *Landolt–Börnstein—Numerical Data and Functional Relationships in Science and Technology*; Lechner, M. D., Ed.; Springer-Verlag: Berlin, Heidelberg, New York, 2009; Vol. VII/25.

Supporting Information

Density, Speed of Sound, and Viscosity Measurements of Reference Materials for Biofuels¹

Arno Laesecke²

Tara J. Fortin²

Jolene D. Splett³

NIST

National Institute of Standards and Technology

²⁾Material Measurement Laboratory
Thermophysical Properties Division

³⁾Information Technology Laboratory
Statistical Engineering Division

325 Broadway
Boulder, CO 80305-3328, U.S.A.

Phone: 1-303-497-3197

Fax: 1-303-497-5224

E-Mail: Arno.Laesecke@Boulder.NIST.Gov

Published in

Energy&Fuels 2012

<http://dx.doi.org/10.1021/ef201645r>

Date of this version: February 7, 2012

¹ Contribution of the National Institute of Standards and Technology. Not subject to Copyright in the U.S.A.

Appendix: Uncertainty Calculations

General	S3
A1 Uncertainty Calculations for the Density Measurements	S4
A2 Uncertainty Calculation for the Speed of Sound Measurements	S7
A3 Uncertainty Calculation for the Viscosity Measurements with the Open Gravitational Capillary Viscometer	S7
A4 Uncertainty Calculation for the Viscosity Measurements with the Rotating Concentric- cylinder Viscometer	S13
A5 References	S16

General

The uncertainty intervals outlined in this document require the assumption that the material is homogeneous. If this assumption is not correct, alternative uncertainty intervals must be used.

There are several equations that are used repeatedly when computing uncertainty. We will provide here a general form of these equations and refer back to them in subsequent sections of the appendix.

The sample standard deviation of n observations is given by

$$s = \sqrt{\frac{\sum_{i=1}^n (x_i - \bar{x})^2}{n-1}}, \quad (\text{A.1})$$

where \bar{x} is the sample mean,

$$\bar{x} = \frac{\sum_{i=1}^n x_i}{n}. \quad (\text{A.2})$$

If the combined standard uncertainty of a measurement result having N influence quantities is

$$u_c(y) = \sqrt{\sum_{i=1}^N (a_i^2 \cdot u(x_i)^2)}, \quad (\text{A.3})$$

where

$$a_i = \frac{\partial y}{\partial x_i}, \quad (\text{A.4})$$

and the influence quantities are independent of each other, then the effective degrees of freedom associated with the combined standard uncertainty can be computed using the Welch-Satterthwaite approximation [A.1, A.2],

$$df = \frac{u_c^4}{\sum_{i=1}^N \frac{a_i^4 \cdot u(x_i)^4}{df_i}}, \quad (\text{A.5})$$

where df_i represents the degrees of freedom for the i^{th} uncertainty component.

The effective degrees of freedom are used to determine the value from the Student's t table needed to compute the expanded uncertainty. In general, the equation for expanded uncertainty is

$$U = t_{1-\alpha/2; df} \cdot u(\gamma), \quad (\text{A.6})$$

corresponding to a $100(1 - \alpha)$ % uncertainty interval. Typically, $\alpha = 0.05$.

A1 Uncertainty Calculations for the Density Measurements

Our best estimate of the certified value of density for the batch of material at a given temperature is the average of n_ρ density measurements. The measurement equation for the average density at a given temperature is

$$\bar{\rho} = \left[\frac{1}{n_\rho} \sum_{i=1}^{n_\rho} \rho_i \right] + C + \gamma, \quad (\text{A1.1})$$

where ρ_i is the i^{th} measured value of density, C is a density correction based on toluene, and γ is the error associated with the resolution of the measurement system based on the manufacturer's specifications. As explained in section 2.1 of this paper, the density correction C applies only to densimeter 1. The combined standard uncertainty is

$$u(\bar{\rho}) = \sqrt{\frac{1}{n_\rho} s_\rho^2 + u^2(C) + u^2(\gamma)}, \quad (\text{A1.2})$$

where s_ρ is the sample standard deviation of n_ρ density measurements (eq. (A.1)), $u(C)$ is the uncertainty of the density correction based on toluene, and $u(\gamma)$ is the uncertainty due to the resolution of the measurement system. For densimeter 1, $u(\gamma) = 0.001 \text{ kg}\cdot\text{m}^{-3}$, while for densimeter 2, $u(\gamma) = 0.1 \text{ kg}\cdot\text{m}^{-3}$. The effective degrees of freedom associated with $u(\bar{\rho})$ are

$$df_\rho = \frac{u^4(\bar{\rho})}{\left[\frac{1}{n_\rho} s_\rho^2 \right]^2 + \frac{u^4(C)}{df_c} + \frac{u^4(\gamma)}{df_\gamma}}, \quad (\text{A1.3})$$

based on the Welch-Satterthwaite approximation, eq. (A.5). There are $n_\rho - 1$ degrees of freedom associated with s_ρ , and we will assume the degrees of freedom associated with $u(\gamma)$ are 30 so that $df_\gamma = 30$. From eq. (A.6), the expanded uncertainty is $U_{\bar{\rho}} = t_{1-\alpha/2; df_\rho} \cdot u(\bar{\rho})$.

The toluene density correction at a given temperature and pressure is

$$C = \rho_{SRM} - \bar{\rho}_M, \quad (\text{A1.4})$$

where ρ_{SRM} is the certified value of density for toluene (NIST SRM 211d) at a specific temperature and pressure, and $\bar{\rho}_M$ is the average density observed for toluene (NIST SRM 211d) based on $m = 5$ observations completed in the laboratory at the same temperature and pressure.

The uncertainty and degrees of freedom associated with the toluene correction C are

$$u(C) = \sqrt{u^2(\rho_{SRM}) + u^2(\bar{\rho}_M)}, \quad (\text{A1.5})$$

and

$$df_C = \frac{u^4(C)}{\frac{u^4(\rho_{SRM})}{df_{SRM}} + \frac{u^4(\bar{\rho}_M)}{df_{\rho_M}}}. \quad (\text{A1.6})$$

The values of, ρ_{SRM} , $u(\rho_{SRM})$ and df_{SRM} are computed as instructed in the certificate of NIST SRM 211d and the related publication by McLinden and Splett [A.3].

The measurement equation for the average value of toluene density is

$$\bar{\rho}_M = \left[\frac{1}{m} \sum_{i=1}^m \rho_{Mi} \right] + \gamma, \quad (\text{A1.7})$$

where ρ_{Mi} is the i^{th} measured value of toluene (SRM 211d) density and γ is the error associated with the resolution of the measurement system based on the manufacturer's specifications. The combined standard uncertainty of $\bar{\rho}_M$ is

$$u(\bar{\rho}_M) = \sqrt{\frac{1}{m} s_{\rho_M}^2 + u^2(\gamma)}, \quad (\text{A1.8})$$

where s_{ρ_M} is the sample standard deviation based on $m - 1$ degrees of freedom. The value of $u(\gamma)$ and its degrees of freedom were defined previously. The degrees of freedom associated with $u(\bar{\rho}_M)$ are computed using the Welch-Satterthwaite approximation, eq. (A.5).

To illustrate the calculations, Tables A1.1 and A1.2 show an example uncertainty budget for NIST SRM 2772 soy-based biodiesel at 10 °C.

Table A1.1: Uncertainty budget for $u(C)$ at 10 °C based on $m = 5$ toluene measurements.

Source	Densimeter 1	
	Uncertainty, kg·m ⁻³	Degrees of Freedom
$u(\bar{\rho}_M) = \sqrt{u^2(\gamma) + \frac{1}{m} s_{\rho M}^2}$	0.0023	5
$u(\gamma)$	0.0010	30
$\frac{1}{\sqrt{m}} s_{\rho M}$	0.0021	4
$u(\rho_{SRM})$	0.031	16
$u(C) = \sqrt{u^2(\rho_{SRM}) + u^2(\bar{\rho}_M)}$	0.031	16

Table A1.2: Uncertainty budget for $u(\bar{\rho})$ at 10 °C based on $n_\rho = 4$ SRM 2772 measurements.

Source	Densimeter 1		Densimeter 2	
	Uncertainty, kg·m ⁻³	Deg. of Freedom	Uncertainty, kg·m ⁻³	Deg. of Freedom
Toluene Correction, $u(C)$	0.031	16		
Measurement Error, $s_\rho / \sqrt{n_\rho}$	0.003	4	0.02	4
Instrument Resolution, $u(\gamma)$	0.001	30	0.10	30
Combined Standard Uncertainty, $u(\bar{\rho})$	0.031	16	0.10	32
<u>Explanation:</u> The information of Table A1.2 can be used to estimate an expanded uncertainty. For example, the average density of the soy-based biodiesel SRM 2772 at 10 °C from densimeter 1 is 888.579 kg·m ⁻³ , the correction for the calibration deviation at the density of toluene is 0.0542 kg·m ⁻³ , and the corrected density is 888.633 kg·m ⁻³ . The expanded uncertainty is 0.066 kg·m ⁻³ based on the coverage factor $k = 2.12$ for a 95 % uncertainty interval and 16 degrees of freedom.				

No calibration correction C is required for measurements with densimeter 2, as is the case for bioethanol AEAC and hydrated bioethanol AEHC in densimeter 1. The uncertainty calculations are simplified because the correction term C and the associated uncertainties can be omitted from the equations. The combined standard uncertainty for densimeter 2 is dominated by the instrument resolution uncertainty.

A2 Uncertainty Calculation for the Speed of Sound Measurements

The uncertainty calculations for the speed of sound measurements are similar to those for the density measurements, except a correction for the calibration deviation at the speed of sound of toluene is not applicable, because toluene is not a standard reference material with regard to its speed of sound. The measurement equation for the average of n_w speed of sound measurements at a given temperature is

$$\bar{w} = \left[\frac{1}{n_w} \sum_{i=1}^{n_w} w_i \right] + \lambda, \quad (\text{A2.1})$$

where w_i is the i^{th} measured speed of sound and λ is the error associated with the resolution of the measurement system based on manufacturer's specifications. The combined standard uncertainty is

$$u(\bar{w}) = \sqrt{\frac{1}{n_w} s_w^2 + u^2(\lambda)}, \quad (\text{A2.2})$$

where s_w is the sample standard deviation based on $n_w - 1$ degrees of freedom. From the manufacturer's specifications of the instrument resolution, $u(\lambda) = 0.1 \text{ m}\cdot\text{s}^{-1}$. We assume there are 30 degrees of freedom associated with $u(\lambda)$. The effective degrees of freedom associated with $u(\bar{w})$ are computed using the Welch-Satterthwaite approximation, eq. (A.5), and the expanded uncertainty is computed according to eq. (A.6).

A3 Uncertainty Calculation for the Viscosity Measurements with the Open Gravitational Capillary Viscometer

The calibration and adjustment of the capillary viscometer involves fitting known kinematic viscosities ν of certified viscosity standards versus measured efflux times τ . Calibration measurements were carried out as described in the main text. We fit efflux time data in the range $40 \text{ s} \leq \tau \leq 110 \text{ s}$. The working equation of the capillary viscometer is

$$\nu = \hat{c} \tau - (\hat{\varepsilon} / \tau^2). \quad (\text{A3.1})$$

The estimates for the capillary constants \hat{c} and $\hat{\varepsilon}$ and their associated uncertainties are listed for each bulb in Table A3.1. The notation with accent circumflex is used to indicate estimates of model parameters, in this case the viscometer constants c and ε . This convention is used in the remainder of the appendix.

Table A3.1: Estimated capillary constants and associated uncertainties to obtain in eq. A3.1 kinematic viscosities in units of $\text{mm}^2\cdot\text{s}^{-1}$ from measured efflux times τ in seconds.

Parameter	Units	Bulb 1	Bulb 2
\hat{c}	$\text{mm}^2\cdot\text{s}^{-2}$	0.086076	0.01052
$u(\hat{c})$	$\text{mm}^2\cdot\text{s}^{-2}$	$43.0\cdot 10^{-6}$	$2.686\cdot 10^{-6}$
$\hat{\varepsilon}$	$\text{mm}^2\cdot\text{s}$	27.0675	61.1251
$u(\hat{\varepsilon})$	$\text{mm}^2\cdot\text{s}$	9.2136	6.8303
$u(\hat{c}, \hat{\varepsilon})$		$2.854\cdot 10^{-4}$	$4.4\cdot 10^{-6}$

The covariance $u(\hat{c}, \hat{\varepsilon})$ listed in Table A3.1 is used to account for the relationship between the two parameters. Information regarding the estimation of the covariance matrix for least-squares parameter estimates is provided in references [A.4] and [A.5].

In our calibration model, the known kinematic viscosity of a certified standard is the dependent variable and the measured efflux time is the independent variable. In least-squares regression, the independent variable is usually “known” and the dependent variable is usually measured. A least-squares regression with errors in the independent variable may have considerable bias in the estimated parameters if the errors are very large. We performed both orthogonal distance regression [A.6, A.7] and least-squares regression of the calibration data. We determined that the errors in efflux time were negligible because the parameter estimates and their uncertainties were very close for both methods. Thus, we use the ordinary least-squares model parameters.

For the measurement of unknown liquids, the appropriate calibration parameters ($\hat{c}, \hat{\varepsilon}$) are used to obtain the viscosity of the sample. From the measurement equation (A3.1), the combined standard uncertainty is

$$u(\nu) = \sqrt{\left(\frac{\partial \nu}{\partial \hat{c}}\right)^2 u^2(\hat{c}) + \left(\frac{\partial \nu}{\partial \hat{\varepsilon}}\right)^2 u^2(\hat{\varepsilon}) + 2\left(\frac{\partial \nu}{\partial \hat{c}}\right)\left(\frac{\partial \nu}{\partial \hat{\varepsilon}}\right)u(\hat{c}, \hat{\varepsilon}) + \left(\frac{\partial \nu}{\partial \tau}\right)^2 u^2(\tau)}. \quad (\text{A3.2})$$

The uncertainties $u(\hat{c})$, $u(\hat{\varepsilon})$, and $u(\hat{c}, \hat{\varepsilon})$ are determined from the least-squares fit of the calibration data.

We typically use the Welch-Satterthwaite approximation to compute the effective degrees of freedom for $u(\nu)$; however, the approximation is only valid if the terms in the uncertainty are

uncorrelated. To obtain independent terms in $u(\nu)$, we must separate our uncertainty into two parts: the three terms associated with the calibration model fit and the term associated with efflux so that

$$u^2(\mathbf{v}_{model}) = \left(\frac{\partial \mathbf{v}}{\partial \hat{\mathbf{c}}}\right)^2 u^2(\hat{\mathbf{c}}) + \left(\frac{\partial \mathbf{v}}{\partial \hat{\mathbf{e}}}\right)^2 u^2(\hat{\mathbf{e}}) + 2\left(\frac{\partial \mathbf{v}}{\partial \hat{\mathbf{c}}}\right)\left(\frac{\partial \mathbf{v}}{\partial \hat{\mathbf{e}}}\right) u(\hat{\mathbf{c}}, \hat{\mathbf{e}}), \quad (\text{A3.3})$$

$$u^2(\mathbf{v}_\tau) = \left(\frac{\partial \mathbf{v}}{\partial \tau}\right)^2 u^2(\tau), \quad (\text{A3.4})$$

and

$$u^2(\mathbf{v}) = u^2(\mathbf{v}_{model}) + u^2(\mathbf{v}_\tau). \quad (\text{A3.5})$$

We can now apply the Welch-Satterthwaite approximation, eq. (A.5), to compute the effective degrees of freedom,

$$df_{\mathbf{v}} = \frac{u^4(\mathbf{v})}{\frac{u^4(\mathbf{v}_{model})}{df_{\mathbf{v}_{model}}} + \frac{u^4(\mathbf{v}_\tau)}{df_\tau}}, \quad (\text{A3.6})$$

where $df_{\mathbf{v}_{model}}$ is the number of observations in the regression fit minus the number of parameters in the model. The expanded uncertainty of $u(\nu)$ is computed according to eq. (A.6).

The calculation of $u(\tau)$ and df_τ will be discussed next. The efflux time measurement equation is

$$\tau = \delta(T) + \theta + \omega, \quad (\text{A3.7})$$

where $\delta(T)$ is the correlated efflux time for a given bath temperature, θ is the repeatability error, and ω represents the manufacturer's specified error in the timing measurement system. The combined standard uncertainty is

$$u(\tau) = \sqrt{u^2(\delta(T)) + \frac{1}{n_\tau} s_\tau^2 + u^2(\omega)}, \quad (\text{A3.8})$$

where s_τ is the sample standard deviation of n_τ efflux measurements, $u(\delta(T))$ is the uncertainty in the correlated efflux for a given bath temperature, and $u(\omega)$ is the uncertainty associated with the

timing measurement system. The term s_x^2/n_x represents the uncertainty due to repeatability error θ .

The value of $u(\omega)$ is given by the measurement system manufacturer as 0.02 s, and we will assume $df_\omega = 30$. The degrees of freedom, df_τ , associated with $u(\tau)$ are computed using the Welch-Satterthwaite approximation, eq. (A.5).

We use empirical models to quantify the relationship between $\delta(T)$ and the bath temperature, T . The models can be used to predict $\delta(T)$ and its associated uncertainty $u(\delta(T))$, for any value of T . The empirical models were generated using commercially available, automated curve fitting and equation discovery software. We selected the simplest possible, three-parameter models that provided the best overall fit to the data based on the residual standard deviation. Adding a fourth parameter did not substantially improve the model fits. The empirical models for each data set and the estimated model parameters and their associated uncertainties are compiled in Table A3.2.

Table A3.2: Empirical models for the relationship between efflux time and bath temperature for each biofuel and bulb with estimated parameter values β_i and their associated uncertainties in parentheses. Units are seconds for $\delta(T)$ and kelvin for temperature T .

Data Set	Bulb	Model $\delta(T) =$	$\hat{\beta}_0(u(\hat{\beta}_0))$	Units	$\hat{\beta}_1(u(\hat{\beta}_1))$	Units	$\hat{\beta}_2(u(\hat{\beta}_2))$	Units
AEAC	2	$[\beta_0 + \beta_1 T^{2.5} + \beta_2 / T^{1.5}]^{-1}$	-0.0331 (0.00051)	s ⁻¹	1.644805×10^{-8} (1.10187×10^{-10})	s ⁻¹ K ^{-2.5}	79.13326 (1.75776)	K ^{1.5} s ⁻¹
AEHC	2	$[\beta_0 + \beta_1 T^2 + \beta_2 T^3]^{-1}$	0.00294 (0.00062556)	s ⁻¹	-3.45051×10^{-7} (1.913072×10^{-8})	s ⁻¹ K ⁻²	1.283609×10^{-9} (4.06588×10^{-11})	s ⁻¹ K ⁻³
SRM2772	1	$[\beta_0 + \beta_1 T + \beta_2 \sqrt{T}]^{-1}$	0.59143 (0.00673)	s ⁻¹	0.00266 (0.00002113)	s ⁻¹ K ⁻¹	-0.07937 (0.00075443)	s ⁻¹ K ^{-0.5}
SRM2772	2	$[\beta_0 + \beta_1 / T^{1.5} + \beta_2 \ln(T) / T^2]^{-1}$	0.05159 (0.00043931)	s ⁻¹	-1248.60588 (14.92470)	K ^{1.5} s ⁻¹	3008.14755 (38.46064)	K ² s ⁻¹
SRM2773	1	$[\beta_0 + \beta_1 T + \beta_2 (\ln(T))^2]^{-1}$	0.71218 (0.00581)	s ⁻¹	0.00181 (0.00000964)	s ⁻¹ K ⁻¹	-0.03811 (0.00026747)	s ⁻¹
SRM2773	2	$[\beta_0 + \beta_1 T + \beta_2 / T^2]^{-1}$	-0.03747 (0.00017420)	s ⁻¹	0.00010144 (3.44533×10^{-7})	s ⁻¹ K ⁻¹	791.54531 (6.52951)	K ² s ⁻¹

We use propagation of errors to determine the value of $u(\delta(T))$. For each three-parameter model, the general form of the squared, standard uncertainty is

$$\begin{aligned}
u^2(\delta(T)) &= \left(\frac{\partial\delta(T)}{\partial\hat{\beta}_0}\right)^2 u^2(\hat{\beta}_0) + \left(\frac{\partial\delta(T)}{\partial\hat{\beta}_1}\right)^2 u^2(\hat{\beta}_1) + \left(\frac{\partial\delta(T)}{\partial\hat{\beta}_2}\right)^2 u^2(\hat{\beta}_2) \\
&+ 2\left(\frac{\partial\delta(T)}{\partial\hat{\beta}_0}\right)\left(\frac{\partial\delta(T)}{\partial\hat{\beta}_1}\right) u(\hat{\beta}_0, \hat{\beta}_1) + 2\left(\frac{\partial\delta(T)}{\partial\hat{\beta}_0}\right)\left(\frac{\partial\delta(T)}{\partial\hat{\beta}_2}\right) u(\hat{\beta}_0, \hat{\beta}_2). \quad (\text{A3.9}) \\
&+ 2\left(\frac{\partial\delta(T)}{\partial\hat{\beta}_1}\right)\left(\frac{\partial\delta(T)}{\partial\hat{\beta}_2}\right) u(\hat{\beta}_1, \hat{\beta}_2) + \left(\frac{\partial\delta(T)}{\partial T}\right)^2 u^2(T)
\end{aligned}$$

To compute the degrees of freedom associated with $u(\delta(T))$, we need to divide $u^2(\delta(T))$ into two parts,

$$\begin{aligned}
u^2(\delta(T)_{\text{model}}) &= \left(\frac{\partial\delta(T)}{\partial\hat{\beta}_0}\right)^2 u^2(\hat{\beta}_0) + \left(\frac{\partial\delta(T)}{\partial\hat{\beta}_1}\right)^2 u^2(\hat{\beta}_1) + \left(\frac{\partial\delta(T)}{\partial\hat{\beta}_2}\right)^2 u^2(\hat{\beta}_2) \\
&+ 2\left(\frac{\partial\delta(T)}{\partial\hat{\beta}_0}\right)\left(\frac{\partial\delta(T)}{\partial\hat{\beta}_1}\right) u(\hat{\beta}_0, \hat{\beta}_1) + 2\left(\frac{\partial\delta(T)}{\partial\hat{\beta}_0}\right)\left(\frac{\partial\delta(T)}{\partial\hat{\beta}_2}\right) u(\hat{\beta}_0, \hat{\beta}_2), \quad (\text{A3.10}) \\
&+ 2\left(\frac{\partial\delta(T)}{\partial\hat{\beta}_1}\right)\left(\frac{\partial\delta(T)}{\partial\hat{\beta}_2}\right) u(\hat{\beta}_1, \hat{\beta}_2)
\end{aligned}$$

and

$$u^2(\delta(T)_{\text{temp}}) = \left(\frac{\partial\delta(T)}{\partial T}\right)^2 u^2(T), \quad (\text{A3.11})$$

so that

$$u^2(\delta(T)) = u^2(\delta(T)_{\text{model}}) + u^2(\delta(T)_{\text{temp}}). \quad (\text{A3.12})$$

The degrees of freedom associated with $u(\delta(T))$ are

$$df_{\delta(T)} = \frac{u^4(\delta(T))}{\frac{u^4(\delta(T)_{\text{model}})}{df_{\delta(T)_{\text{model}}}} + \frac{u^4(\delta(T)_{\text{temp}})}{df_{\delta(T)_{\text{temp}}}}}. \quad (\text{A3.13})$$

Eqs. (A3.12) and (A3.13) are analogous to eqs. (A3.5) and (A3.6) in the previous section. The uncertainties in the estimated model parameters are easily obtained from the regression fit, and $df_{\delta T_{\text{model}}}$ is the number of observations used in the regression fit minus the number of parameters in the model. The uncertainty in the temperature measurement, $u(T)$ is a type B uncertainty [A.1, A.2] defined as the combination of manufacturer's specified error, long-term fluctuations in the bath temperature, and uncertainty due to the distance from the thermometer to the bulb. The uncertainty due to manufacturer's specified error and the uncertainty due to the bath temperature are both 0.01 K. The uncertainty due to the distance from the thermometer to the capillary is thought to increase linearly from 0.02 K at 20 °C to 0.1 K at 100 °C so that the uncertainty is $0.001 \text{ K} \cdot (\text{°C})^{-1} \cdot t$ where t is the temperature in °C. We estimate the temperature uncertainty to be

$$u(T) = \sqrt{(0.01)^2 + (0.01)^2 + (0.001 \cdot t)^2}, \quad (\text{A3.14})$$

We will assume that we have a fairly high degree of confidence in our estimate of $u(T)$ so that $df_{\delta T_{\text{temp}}} = 30$. The value of $df_{\delta T}$ from eq. (A3.13) is used to obtain the expanded uncertainty $u(\nu)$ for measurements with the capillary viscometer according to eq. (A.6).

A4 Uncertainty Calculation for the Viscosity Measurements with the Rotating Concentric-cylinder Viscometer

In this instrument, the measurement equation for dynamic viscosity at a given temperature is

$$\eta = f(T) + \kappa + \phi, \quad (\text{A4.1})$$

where $f(T)$ is a correlation of the temperature dependence of the measured dynamic viscosities to assess the uncertainty of the viscosity due to the uncertainty of the temperature measurement. The quantity κ is the repeatability error, and ϕ is the error associated with the resolution of the measurement system based on manufacturer's specifications. No other quantities of influence could be included in the analysis because details of the measurement system are not disclosed by the manufacturer. The combined standard uncertainty associated with the dynamic viscosity η is

$$u(\eta) = \sqrt{u^2(f(T)) + \frac{1}{m_\eta} s_\eta^2 + u^2(\phi)}, \quad (\text{A4.2})$$

where $u(f(T))$ is the uncertainty of the correlated dynamic viscosity, s_η is the sample standard deviation of m_η observations, and $u(\phi)$ is the uncertainty due to the manufacturer's specified error in the measurement system. The term s_η^2 / m_η represents the uncertainty due to repeatability error κ .

The effective degrees of freedom associated with $u(\eta)$ are computed using the Welch-Satterthwaite approximation, eq. (A.5), and the expanded uncertainty is computed as given by eq. (A.6).

The instrument repeatability specified by the manufacturer is $\pm 0.1\%$ of the measured value. The manufacturer's specifications only provide limits to error, so these limits must be converted to a standard deviation based on procedures outlined in reference [A.1]. Assuming that the limits to error represent bounds to a uniform distribution, then

$$u(\phi) = \frac{0.001 \cdot \eta_i}{\sqrt{3}}. \quad (\text{A4.3})$$

Since $u(\phi)$ depends on the value of viscosity, we use $\eta_i = \eta_{\max}$ to obtain a conservative estimate of $u(\phi)$. We will assume there are 30 degrees of freedom associated with $u(\phi)$ so that $df_\phi = 30$.

We use again empirical models to quantify the relationship between dynamic viscosity and temperature. Note that wider temperature ranges were measured with viscometer 2 than with viscometer 1. Here, the dynamic viscosity data of all four biofuels could be represented by the same empirical model

$$f(T) = \left[\frac{\alpha_0 + \alpha_1 T}{1 + \alpha_2 T} \right]^2. \quad (\text{A4.4})$$

The estimated model parameters and their uncertainties for each of the four biofuels are given in the following table.

Table A4.1: Estimated values of the parameters in eq. (A4.4) and associated uncertainties (shown below the estimates in parentheses) for each of the biofuels. Units are mPa·s for $f(T)$ and kelvin for temperature T .

	$\hat{\alpha}_0(u(\hat{\alpha}_0))$	$\hat{\alpha}_1(u(\hat{\alpha}_1))$	$\hat{\alpha}_2(u(\hat{\alpha}_2))$
Data Set	(mPa·s) ^{0.5}	(mPa·s) ^{0.5} ·K ⁻¹	K ⁻¹
AEAC	-2.02292 (0.03020)	0.003091156 (0.00006700)	-0.006880761 (0.00003300)
AEHC	-1.32496 (0.010200)	0.001926756 (0.00002500)	-0.005515964 (7.731×10 ⁻⁶)
SRM 2772	-0.69677 (0.00777)	-0.000313439 (0.00001800)	-0.004541126 (3.8×10 ⁻⁶)
SRM 2773	-0.72848 (0.00404)	-0.000189247 (9.316×10 ⁻⁶)	-0.004479197 (1.784×10 ⁻⁶)

The uncertainty of the correlated viscosity is

$$\begin{aligned}
u^2(f(T)) &= \left(\frac{\partial f(T)}{\partial \hat{\alpha}_0}\right)^2 u^2(\hat{\alpha}_0) + \left(\frac{\partial f(T)}{\partial \hat{\alpha}_1}\right)^2 u^2(\hat{\alpha}_1) + \left(\frac{\partial f(T)}{\partial \hat{\alpha}_2}\right)^2 u^2(\hat{\alpha}_2) \\
&+ 2\left(\frac{\partial f(T)}{\partial \hat{\alpha}_0}\right)\left(\frac{\partial f(T)}{\partial \hat{\alpha}_1}\right)u(\hat{\alpha}_0, \hat{\alpha}_1) + 2\left(\frac{\partial f(T)}{\partial \hat{\alpha}_0}\right)\left(\frac{\partial f(T)}{\partial \hat{\alpha}_2}\right)u(\hat{\alpha}_0, \hat{\alpha}_2). \quad (\text{A4.5}) \\
&+ 2\left(\frac{\partial f(T)}{\partial \hat{\alpha}_1}\right)\left(\frac{\partial f(T)}{\partial \hat{\alpha}_2}\right)u(\hat{\alpha}_1, \hat{\alpha}_2) + \left(\frac{\partial f(T)}{\partial T}\right)^2 u^2(T)
\end{aligned}$$

The parameter uncertainty estimates are available from the regression fit, and $u(T)$ is given as 0.02 K.

To obtain independent terms in $u(f(T))$ we must separate our uncertainty into two parts: the six terms associated with the model fit

$$\begin{aligned}
u^2(f(T)_{\text{model}}) &= \left(\frac{\partial f(T)}{\partial \hat{\alpha}_0}\right)^2 u^2(\hat{\alpha}_0) + \left(\frac{\partial f(T)}{\partial \hat{\alpha}_1}\right)^2 u^2(\hat{\alpha}_1) + \left(\frac{\partial f(T)}{\partial \hat{\alpha}_2}\right)^2 u^2(\hat{\alpha}_2) \\
&+ 2\left(\frac{\partial f(T)}{\partial \hat{\alpha}_0}\right)\left(\frac{\partial f(T)}{\partial \hat{\alpha}_1}\right)u(\hat{\alpha}_0, \hat{\alpha}_1) + 2\left(\frac{\partial f(T)}{\partial \hat{\alpha}_0}\right)\left(\frac{\partial f(T)}{\partial \hat{\alpha}_2}\right)u(\hat{\alpha}_0, \hat{\alpha}_2), \\
&+ 2\left(\frac{\partial f(T)}{\partial \hat{\alpha}_1}\right)\left(\frac{\partial f(T)}{\partial \hat{\alpha}_2}\right)u(\hat{\alpha}_1, \hat{\alpha}_2)
\end{aligned} \tag{A4.6}$$

and the term associated with temperature

$$u^2(f(T)_{\text{temp}}) = \left(\frac{\partial f(T)}{\partial T}\right)^2 u^2(T), \tag{A4.7}$$

so that

$$u^2(f(T)) = u^2(f(T)_{\text{model}}) + u^2(f(T)_{\text{temp}}) \tag{A4.8}$$

The degrees of freedom associated with $u(f(T))$ are

$$df_{f(T)} = \frac{u^4(f(T))}{\frac{u^4(f(T)_{\text{model}})}{df_{f(T)\text{model}}} + \frac{u^4(f(T)_{\text{temp}})}{df_{f(T)\text{temp}}}}. \tag{A4.9}$$

The value of $df_{f(T)\text{model}}$ is the number of observations in the regression fit minus the number of parameters. We will assume the manufacturer's specified error in temperature is well known so that there are 30 degrees of freedom associated with this term ($df_{f(T)\text{temp}} = 30$). The value of $df_{f(T)}$ from eq. (A4.9) is used to obtain the expanded uncertainty $u(\eta)$ for measurements with the rotating concentric-cylinder viscometer according to eq. (A.6).

A5 References

- [A.1] International Organization for Standardization, Guide to the Expression of Uncertainty in Measurement, International Organization for Standardization, Geneva Switzerland, 1993 (corrected and reprinted 1995).
- [A.2] Taylor, B. N., and Kuyatt, C. E., "Guidelines for Evaluating and Expressing the Uncertainty of NIST Measurement Results," NIST Technical Note 1297, 1994 Edition, (<http://physics.nist.gov/cuu/Uncertainty/>).

- [A.3] McLinden, M. O. and Splett, J. D., "A Liquid Density Standard Over Wide Ranges of Temperature and Pressure Based on Toluene," *NIST Journal of Research*, Vol. 113, No. 1, 2008, pp. 29-67 (<http://nvl.nist.gov/pub/nistpubs/jres/113/1/cnt113-1.htm>).
- [A.4] Seber, G. A. F., *Linear Regression Analysis*, John Wiley & Sons, New York, NY, 1977.
- [A.5] de Levie, R., *Advanced Excel® for Scientific Data Analysis*, Oxford University Press, Oxford, UK, 2004.
- [A.6] Boggs, P. T., Byrd, R. H., Rogers, J. E. and Schnabel, R. B. (1992). User's Reference Guide for ODRPACK Version 2.01 Software for Weighted Orthogonal Distance Regression (National Institute of Standards and Technology, NISTIR 4834, Gaithersburg, MD, <http://gams.nist.gov>).
- [A.7] Zwolak, J. W., Boggs, P. T. and Watson, L. T., "ODRPACK95: A Weighted Orthogonal Distance Regression Code with Bound Constraints," *ACM Transactions on Mathematical Software (TOMS)*, Vol. 33, Issue 4, August 2007.